ORNL/TM-2016/748

DN/DG Screening of Environmental Swipe Samples: FY2016 Report

Stephen Croft
Ramkumar Venkataraman
Robert McElroy
Justin Knowles
David Glasgow

01/28/2017

OAK RIDGE NATIONAL LABORATORY
MANAGED BY UT-BATTELLE FOR THE US DEPARTMENT OF ENERGY

ORNL/TM-2016/748

Nuclear Security and Isotope Technology Division

DN/DG Screening of Environmental Swipe Samples: FY2016 Report

Stephen Croft
Ramkumar Venkataraman
Robert McElroy
Justin Knowles
David Glasgow

Date Published:
01/28/2017

Prepared by
OAK RIDGE NATIONAL LABORATORY
Oak Ridge, TN 37831-6283
managed by
UT-BATTELLE, LLC
for the
US DEPARTMENT OF ENERGY
under contract DE-AC05-00OR22725

CONTENTS

ABSTRACT

The Delayed Neutron Delayed Gamma (DNDG) technique provides a new analytical capability to the International Atomic Energy Agency (IAEA) for detecting undeclared nuclear activities. IAEA's Long Term R&D (LTRD) plan has a stated high urgency need to develop elemental and isotopic signatures of nuclear fuel cycle activities and processes (LTRD 2.2). The new DNDG capability is used to co-detect both uranium and plutonium as an extension of a DN only method that is already being utilized by the IAEA for the analysis of swipes to inform on undeclared nuclear activities. Analytical method involving irradiation of swipe samples potentially containing trace quantities of fissile material in a thermal neutron field, followed by the counting of delayed neutrons, is a well-known technique in the field of safeguards and nonproliferation. It is used for detecting the presence of microscopic amounts of fissile material, (typically a linear combination of ^{233}U, ^{235}U, ^{239}Pu, and ^{241}Pu)and quantifying it in terms of the equivalent mass of ^{235}U. The delayed neutron (DN) technique is very sensitive and is been routinely employed at the High Flux Isotope Reactor (HFIR) facility at Oak Ridge National Laboratory (ORNL). Both uranium and plutonium are of high safeguards value. However, the DN technique is not well suited for distinguishing between U and Pu isotopes since the decay curves overlap closely. The delayed gamma (DG) technique will help detect the presence of ^{239}Pu in a mixture of U and Pu. Thus the DNDG approach combines the best of both worlds; the sensitivity of DN counting and the isotopic specificity of DG counting. The present work seeks to build on the delayed neutron and delayed gamma methods that have been developed at ORNL. It is recognized that the distribution profile of heavy fission products remains fairly invariant for the fissile nuclides whereas the distribution of light fission products varies from one isotope to another. That is, the ratio of the yield of a light fission fragment to a heavy fission fragments is isotope specific. Measurement of the ratio of the net full energy peak (FEP) from low/high mass fission products is an elegant way to characterize the fraction of fissile materials present in a mixture. By empirically calibrating the ratio of the net FEP as a function of known concentration of the binary mixture, one can determine the fraction of fissile isotopes in an unknown sample. In the work done in fiscal year (FY) 2016, samples of single fissile material isotopes as well as binary mixtures were irradiated in a well thermalized irradiation field in the HFIR. Delayed neutron counting was performed using the neutron counter at the HFIR Neutron Activation Analysis (NAA) laboratory. Delayed gamma counting was performed using a shielded high purity germanium (HPGe) detector. Delayed neutron decay curve results highlighted the difficulty of distinguishing between U and Pu isotopes, and the need for including the delayed gamma component. Based on delayed gamma spectrometry, twelve ratios of low mass/high fission product gamma ray FEP have been identified as valid candidates. Linearity of the ratios, as a function of ^{239}Pu fraction in ^{235}U+^{239}Pu mixtures, was confirmed for the low mass/high mass candidates that were selected. The DNDG method we are spearheading allows not only the presence of total fissile content to be detected, but whether the material is predominantly U or predominantly Pu, or a mixture. This provides additional SG relevant information.

1. INTRODUCTION

The Neutron Activation Analysis Facility (NAAF) at the High Flux Isotope Reactor (HFIR) offers two pneumatic transfer systems (PT-1 and PT-2) that accomplish neutron irradiation and also delayed neutron (DN) measurement in support of Laboratory Challenge exercises, International Atomic Energy Agency (IAEA) pre-inspection check swipe analysis, fissile material quantification, and elemental characterization for nuclear forensics missions. These specialized techniques offer nondestructive analysis of materials at the nanogram level and below. Delayed neutron activation analysis (DNAA) remains one of the most sensitive methods when it comes to assaying single-isotope fissile material samples [1], [2]. At ORNL, the technique is especially attractive because the pneumatic transfer systems are the best in the world. Preliminary work at the HFIR-NAA facility has shown great promise for the characterization of

samples containing fissile materials using both neutrons and gamma rays from short lived fission products [3] [4]. Glasgow et al. [3] have achieved a sensitivity of 15 picograms for ^{235}U using DNAA. Kapsimalis et al. [4] have developed an analytical method that would allow the concentrations of mixtures of trace amounts of ^{235}U and ^{239}Pu to be determined from a single delayed neutron emission profile of an irradiated sample to within 5 to 10%. Kapsimalis et al. used a multivariate linear regression model to describe the delayed neutron emission profile of an irradiated sample for the concurrent determination of the two fissile nuclides in the sample. Trying to distinguish between individual fissile isotopes using delayed neutron counting alone depends on how well the decay curves of the fissile isotopes can be fit and on how they are normalized, more fundamentally on the group structure and on the irradiation and count cycle. More recently, Knowles et al. [5] developed a delayed gamma-based method where fission product photopeak yields are used to construct an overdetermined system of linear equations and solve for each of the original fissile isotope masses. Knowles' method seeks to determine the fission product fields from an irradiated sample using SCALE-ORIGEN [6] simulations. Absolute quantities such as the neutron spectrum and magnitude, the induced fission reaction cross sections, and the absolute efficiency of the gamma-ray detector are needed as inputs. The method is capable of mass recoveries with biases less than 7%, and with a propagated uncertainty of less than 10%.

The present work seeks to build on the individual delayed neutron and delayed gamma methods that have been developed at ORNL. In the present work, it is recognized that the distribution of fission products created following neutron-induced fission of different fissile isotopes varies over a wide range. The distribution profile of heavy fission products remains fairly invariant for the fissile nuclides. However, the distribution of light fission products varies from one isotope to another (Figure 1). That is, the ratio of light fission fragments to heavy fission fragments is different for different fissile species such as ^{235}U, ^{239}Pu, ^{233}U, etc. Measurement of the ratio of the net full energy peak (FEP) from high/low mass fission products offers an attractive analytical way to characterize the fraction of fissile materials present in a mixture. By empirically calibrating, by direct measurement, the ratio of the net FEP as a function of known concentration of the binary mixture, one can determine the fraction of fissile isotopes in an unknown sample. Empirical calibration frees us from uncertainties in basic nuclear data and is naturally inclusive of secondary effects such as spectral differences between the emission spectra of the various delayed neutron groups. Measuring ratios rather than absolute quantities reduces systematic uncertainties such as those in rate loss corrections and in efficiency calibration. The fissile isotope fractions determined from delayed gamma measurements can be combined with the ^{235}U equivalent quantitative mass results from delayed neutron measurements to determine isotope specific masses present in the analyzed sample.

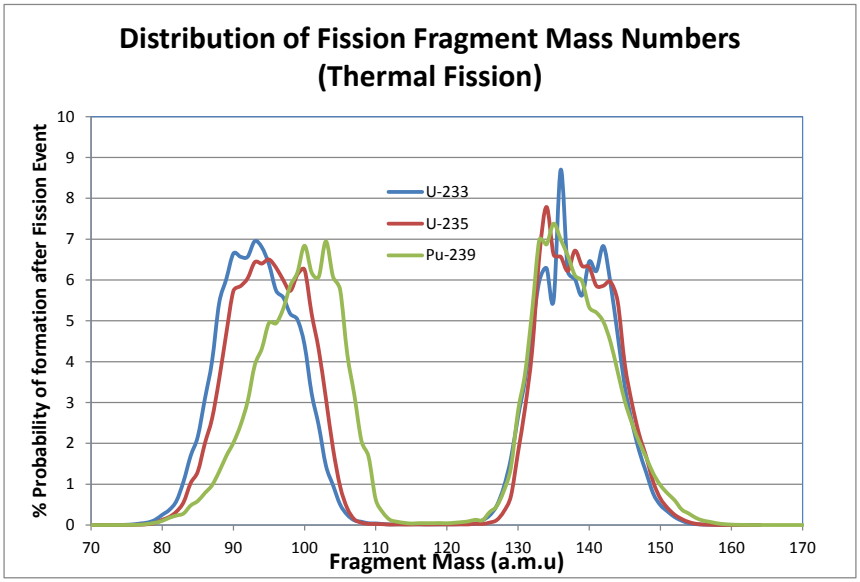

Figure 1. Distribution of Fission Fragment Mass Numbers

Table 1 shows a simple comparison of the HFIR-NAA capabilities for low detection limits and rapid analysis periods.

Table 1: Knowles et al. experiments at HFIR-NAA show potential for low detection limts using Short Lived Fission Product (SLFP) gamma rays

	Fissile Mass Evaluated	**Analysis Time**	**Neutron Spectrum**
Marrs et al. [3]	0.19 – 0.57 g	10 – 840 min	14 MeV + Thermal
Beddingfield et al. [4]	40 g	26 min	Moderated ^{252}Cf
Andrews et al. [5]	$1.3 \cdot 10^{-6}$ – $4.3 \cdot 10^{-6}$ g	< 5 min	Thermal
Knowles et al. [2]	$1.2 \cdot 10^{-8}$ – $1.2 \cdot 10^{-7}$ g	< 10 min	Thermal

2. DNDG METHODLOGY

The DNDG methodology involves the irradiation of a sample consisting of trace quantities (nanograms) of U and Pu isotopes collected on a benign matrix, in a well thermalized neutron field, and after a *minimal* delay time, counting the delay neutrons first, and then counting delayed gammas emitted by short lived fission products. Delayed gamma spectroscopy is used to measure the fraction of fissile isotopes present in a sample by comparing the ratio of low and high mass short-lived fission products. By empirically calibrating the ratio of net full energy peak areas as a function of known concentration of the binary mixture (e.g. ^{235}U+^{239}Pu), the fraction of fissile isotopes in an unknown sample is determined. In order to quantify individual isotopic masses the gamma-ray results are combined with the ^{235}U equivalent mass determined by DN counting. Our focus is on developing a sensitive and robust tool that can be applied routinely with high throughput.

The equations governing DN and DG counting are presented in this section. The sample containing fissile material(s) is irradiated in one of HFIR's pneumatic tube (PT) facilities, PT1 or PT2, for a time period t_{irr}. After the irradiation stops, precursor production ceases, and the activity produced decays with decay constant λi. After a period of delay, t_{dly}, after the end of the irradiation, a count of duration, t_{cnt},is begun using a neutron counter with an efficiency of ε_i counts per delayed neutrons emitted. The net number of events recorded, assuming negligible counter dead-time losses, is therefore the sum over all delayed neutron groups.

$$C = m\frac{N_A\sigma_f}{A}\varphi\sum_{flux}\sum_{i=1}^{n_{grp}}\varepsilon_i\frac{\beta_i}{\lambda_i}\left(1-e^{-\lambda_i t_{irr}}\right)e^{-\lambda_i t_{dly}}\left(1-e^{-\lambda_i t_{cnt}}\right),\ counts \qquad (1)$$

In equation, m is the mass of the fissile isotope, ϕ is the neutron flux, σ_f is the induced fission reaction cross section, A is the atomic weight of the fissile isotope, N_A is the Avogadro number, and βi is the fraction of fissions that result in delayed neutron production with the decay constant λ_i in units of s^{-1}. This is our fundamental predictive (or causal relation) physical model equation for delayed counting in the case of a single fissioning species subjected to a single irradiation-delay-count cycle. It can be used in various ways: for example, in an absolute sense to explore nuclear data parameters; inverted (or solved) for the flux; solved for the mass of the fissile material in unknown samples relative to known calibration measurements; or used to formulate uncertainty quantification. In the present work we adopt the eight-group (n_{grp} = 8) model developed by the Nuclear Energy Agency working group [7]. The half-lives of the

eight delayed precursor groups and the delayed neutron yields β (neutrons/fission) are given in Table 2 for ready reference.

Table 2. Eight-Group Representation of Delayed Neutron Precursors [7]

DN Group	Half-life (s)	DN Yield (β) ^{233}U	DN Yield (β) ^{235}U	DN Yield (β) ^{239}Pu	DN Yield (β) ^{241}Pu	DN Yield (β) ^{252}Cf	DN Yield (β) ^{238}U
1	55.6	0.000534	0.000531	0.000208	0.000256	0.00012	0.000391
2	24.5	0.001119	0.002494	0.001541	0.002801	0.002735	0.004836
3	16.3	0.001005	0.001474	0.000537	0.00088	8.6E-06	0.001744
4	5.21	0.00134	0.003192	0.001183	0.002721	0.001797	0.006371
5	2.37	0.001997	0.00536	0.001912	0.004482	0.00172	0.013671
6	1.04	0.00026	0.001462	0.000531	0.002657	0.001238	0.009207
7	0.424	0.000375	0.001316	0.000468	0.001809	0.00098	0.005952
8	0.195	7.04E-05	0.000371	0.00012	0.000392	0	0.004329

The irradiation scheme sequence is illustrated in Figure 2.

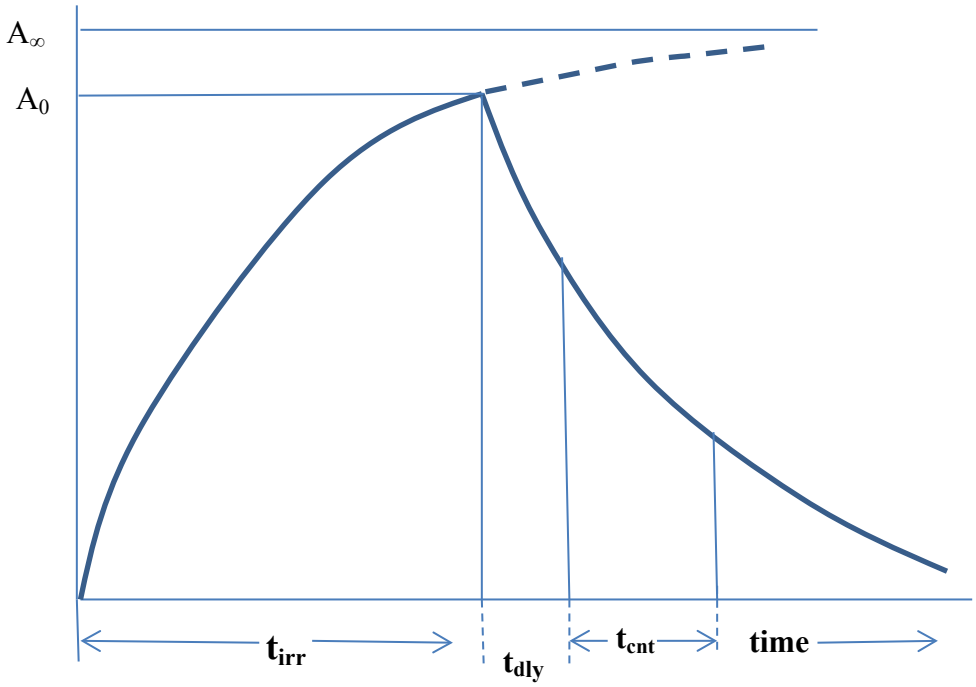

Figure 2. Irradiation scheme

The ORNL DN system is operated in a comparative mode in which it is not possible to quantify both plutonium and uranium in the same sample. Instead, total fissile content is reported as ^{235}U equivalents in mixed samples and is derived from comparing the total counts to those from a uranium comparator [3]. Using a comparator method eliminates the need to know quantities such as the neutron flux, the neutron spectrum, the reaction cross section, the detector efficiency the delayed neutron yields and the half-lives of the delayed neutron groups.

For DN counting, the shorter the time delay after the end of irradiation, the better, since otherwise the shorter lived precursor groups will decay away and not contribute to the count rate profile. For the irradiations performed in the current work, the time delay was 3 seconds.

The governing equation for DG counting of an irradiated sample with a single fissile isotope is given by equation (2).

$$C_i = m\frac{N_A\sigma_f}{A}\varphi\varepsilon_i\Gamma_i\frac{Y_i}{\lambda_i}\left(1-e^{-\lambda_i t_{irr}}\right)e^{-\lambda_i t_{dly}}\left(1-e^{-\lambda_i t_{cnt}}\right),\ counts \qquad (2)$$

In equation (2), C_i is the net FEP counts from a gamma ray "i", Γ is number of gamma rays emitted per decay of the fission product, ε_γ is the full energy peak efficiency of the gamma-ray detector at the gamma-ray energy of interest, and Y_γ is the fission product yield.

Based on equation (2), one can write down the ratio of FEP counts from gamma rays emitted by a low mass fission product to a high mass fission product. For example, equation (3) gives the ratio for a binary mixture of ^{235}U and ^{239}Pu.

$$\frac{C_{low}}{C_{high}} = \frac{m_{235} * K_{235-low} * Y_{235-low} + m_{239} * K_{239-low} * Y_{239-low}}{m_{235} * K_{235-high} * Y_{235-high} + m_{239} * K_{239-high} * Y_{239-high}} \qquad (3)$$

The K factors consist of parameters that are specific to a given fissile isotope, and to a specific gamma ray emitted by a given fission product. As an example, the K factor for a low mass fission product from the induced fission of ^{235}U is given in equation (4).

$$K_{235-low} = \frac{\sigma_{f-235}}{A_{235}} * \frac{\varepsilon_{235-low} * \Gamma_{235-low}}{\lambda_{235-low}}\left(1-e^{-\lambda_{235-low}t_{irr}}\right)e^{-\lambda_{235-low}t_{dly}}\left(1-e^{-\lambda_{235-low}t_{cnt}}\right) \qquad (4)$$

Note that parameters such as the neutron flux ϕ and the Avogadro number N_A cancel out of equation (3) since they are common to all of the terms in the numerator and the denominator.

Equation (3) provides an insight into the dependence of the FEP count ratio on various parameters including the mass (or concentration) of the fissile isotopes in the mixture and the fission product yields. For a given low and high mass fission product pair, and gamma rays emitted by them, the FEP count ratio will vary as a function of the mass or concentration of the fissile isotopes in the sample. In the practical application of the method for the U-Pu mixture, the FEP count ratio is empirically calibrated as a function of the relative concentration (we use mass ratio) of ^{239}Pu from 0% to 100% in the ^{235}U+^{239}Pu mixture. The calibration data points are fit using a suitable functional form. The relative concentration of ^{239}Pu in an unknown sample is determined by measuring the ratio of the FEP counts from gamma rays emitted by a given low and high mass fission products. The isotopic specificity of this method depends on the selection of fission products that have a high yield for one of the isotopes in the mixture, (e.g.) ^{239}Pu, and can therefore be used to flag the presence of ^{239}Pu.

3. EXPERIMENTAL SETUP

The HFIR-NAA facility contains unique array of capabilities to test the creation and subsequent measurement of short-lived fission product gamma rays. The combination of a high thermal flux and fast-transfer pneumatic tube access allows for some of the lowest detection limits for fissile isotopes using NDA methods to be obtained. The two pneumatic tubes (PT-1 and 2) at the NAA laboratory enter the core at the VXF-7 position in the outer beryllium and the EF-2 position which is peripheral to the outer

beryllium. PT-1 and 2 achieve thermal neutron fluxes of about $4 \cdot 10^{14}$ and $4 \cdot 10^{13}$ n/cm^{2}s, with a thermal-to-epithermal ratio of about 45 and 250, respectively (see 3). The consistency of these neutron fluxes are monitored daily using activated Au and Mn diluted in aluminum foil.

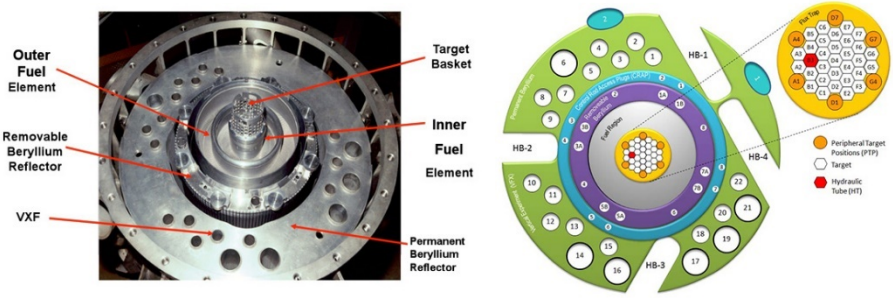

Figure 3: HFIR Core Diagram

For samples containing uranium, the highly thermalized flux in these irradiation positions is advantageous for simplifying the fissile mass characterization. While neutron-induced fission is the dominant reaction in ^{235}U, neutron absorption dominates for ^{238}U. This allows for a simple quantification of ^{238}U mass through neutron activation analysis via ^{239}U gamma-ray measurements (at 74 keV). In addition, the NAA laboratory contains a hot cell, fume hoods, delayed neutron counting station, and multiple HPGe detectors for sample preparation and measurement. This combination of high neutron flux and nearby counting equipment allows for rapid irradiations and measurements of trace quantities of fissile isotopes (see Figure 4).

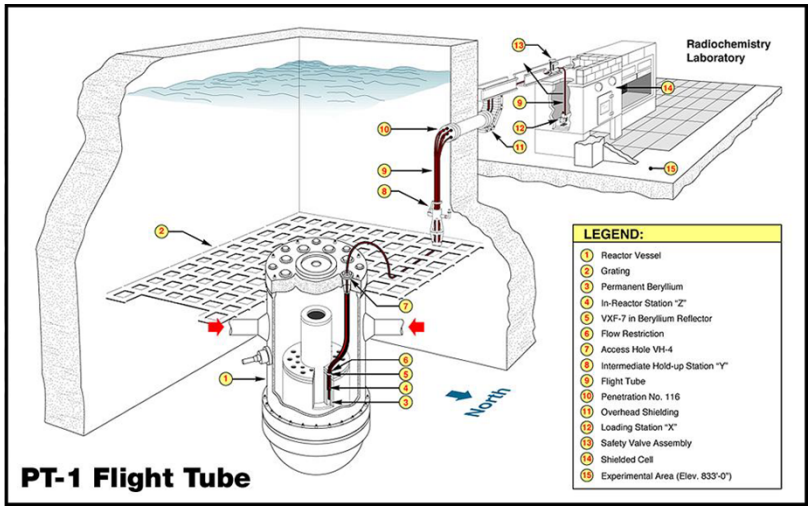

Figure 4: PT-1 Flight Tube Diagram (PT-2 has similar layout)

3.1 DELAYED NEUTRON COUNTER

The DN counter at the HFIR NAA laboratory [3] consists of 18 ^{3}He proportional tubes, embedded in polyethylene (Figure 5a). Each tube has a diameter of 5 cm and an active length of 30 cm. The fill pressure of ^{3}He in each tube is 5 atm. Polyethylene moderator surrounds the detectors and flight tube and forms a cube approximately 45.72 cm (18 inches) in each dimension. Lead shielding, 5.08 cm (2 inches)

thick, is molded around the flight tube and air exit line at the counting position to provide personnel shielding.

The counter consists of a 10.16 cm (4 inch) thick layer of borated polyethylene to shield against neutron background (there is an experimental beam line in the room below), surrounded by an outer layer of 5.08 cm (2 inch) thick lead to reduce the external gamma ray background. The counter 18 ^{3}He proportional tubes are arranged in two concentric rings, and configured into three groups (indicated as green, yellow, and pink in Figure 5a) of 6 tubes each (similar efficiency and dead time). The aggregate signal of each group is amplified and converted to a digital signal. Bias is typically +1400 V to +1500 V and is applied to all six detectors in a group through a manifold which contains a capacitor for smoothing. Total counts for each detector group are obtained from a 3-channel scalar that also controls counting time.

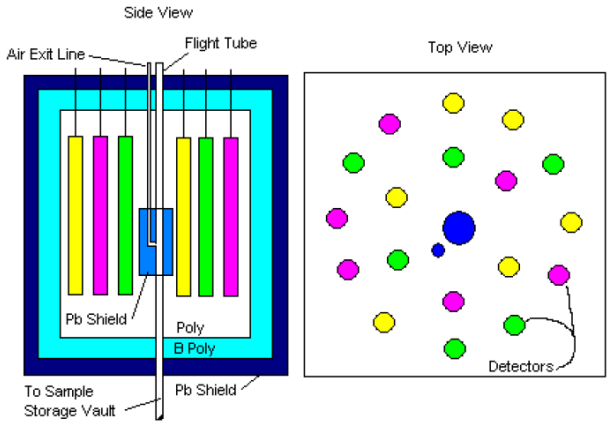

Figure 5a. Schematic drawing of the DN Counter at the HFIR NAA laboratory

High density polyethylene sample containers ("rabbits") were used to transport each (swipe) sample into the reactor for an irradiation using PT-2. Upon exiting the reactor, the samples are brought back to the center of the DN counter cavity. The rabbit is held in the counter according the diagram shown in Figure 5b. Counter-current air columns move the rabbit to the place where the tube is vented. In figure 5b, the vent tube is shown in addition to the rabbit tube. The vent is connected to a valve which remains open during counting. As long as the valve is open, the rabbit will remain in the counting position. The drawing in figure 5b describes the scenario at the reactor mid-plane, but the same description is applicable to the counting position. The rabbit covers the vent port.

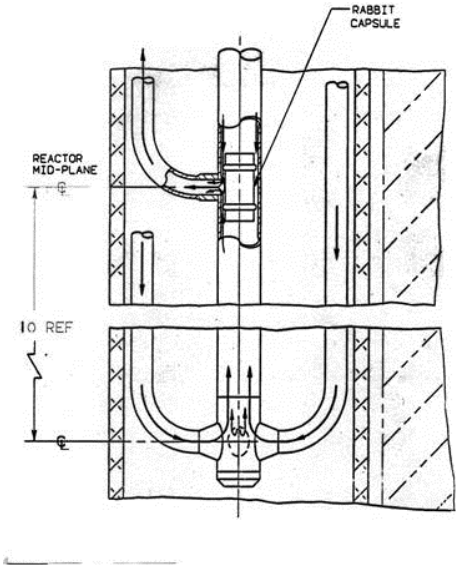

Figure 5b. Mechanism to hold the rabbit in counting position

3.2 DELAYED GAMMA COUNTING SET UP

For this series of experiments, a mechanically cooled High Purity Germanium (HPGe) detector with an Integrated Cryo-Cooling System (ICS) supplied by ORTEC [8] was used. The HPGe with the ICS is a p-type coaxial detector with a relative efficiency of 44% and an energy resolution of 1.9 keV Full Width at Half Maximum (FWHM) at 1332 keV. During the early stages of the measurement campaign, a liquid nitrogen cooled Canberra Broad Energy Germanium (BEGe) detector model BE3825 was considered. The BEGe detector was transported from the ORNL safeguards laboratory to the HFIR NAA lab (FY16 Task 2). The energy resolution of the BE3825 was slightly better (1.8 keV FWHM at 1332 keV) than the p-type coaxial detector. However, its relative efficiency is approximately 26% which is less than that of the ICS HPGe. Also, the fission product gamma energies that were candidates for the DG analysis happened to be mostly above 200 keV or so. So, the superior resolution performance offered by the BEGe detector was not important in this work. The attenuation of the low energy gamma rays and the lead X-rays by the front dead layer of the p-type coaxial detector is also beneficial since it helps to reduce the system dead time (the BEGe would require a filter). Taking into consideration all of the above reasons, and the logistics of transporting the BEGe back and forth from the safeguards lab, it was decided that the the ICS p-type coaxial detector in the HFIR NAA laboratory would be the most suitable for the DNDG work.

The HPGe detector was shielded by 2.54 cm (1 inch) thick lead blocks on all sides. The detector was not collimated. The shielded HPGe detector was set up to count the sample placed on-axis with respect to the detector, at a distance of 32.5 cm. The source to detector distance was dictated by considerations such as avoiding excessive dead time (> 35%) and random summing, avoiding true coincidence summing effects, and space constraints in the laboratory. The shielded HPGe detector set up is shown in Figure 6.

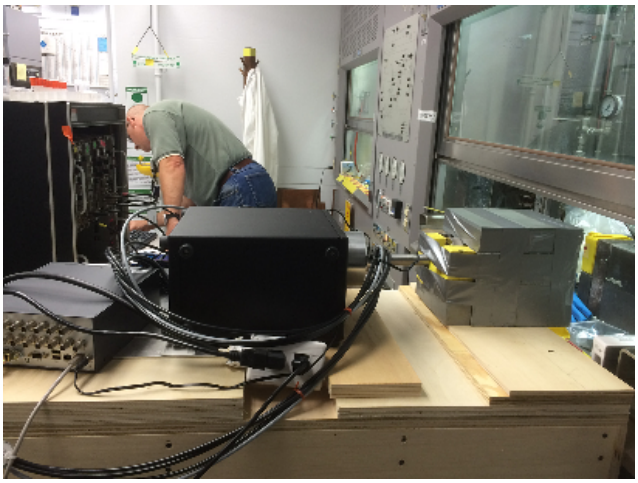

Figure 6. Shielded HPGe detector for DG measurements

The gamma spectroscopy software used for acquisition and analysis was Canberra's Genie 2000. The multi-channel analyzer (MCA) used in these experiments was a Canberra Lynx digital MCA [9] with 16,384 channels operated in Dual Loss Free Counting (DLFC) mode.

DLFC allows for the real-time acquisition of events, and divides the 32,768 available channels to produce two spectra. One spectrum contains live time corrected counts, and the other produces the normal uncorrected counts. This allows for uncertainty to be derived from the uncorrected spectrum, due to the non-Poisson nature of the corrected spectrum [9]. For the experiments described in this work, the majority of fission product isotopes measured experience at least one half-life over the period of measurement and dead-times range between 10% and 35%. These conditions make DLFC mode of unique utility in making an accurate measurement of a decaying fission product's activity during count. Efforts were taken at the HFIR-NAA facility to validate the accuracy (low bias) of DLFC mode with known sources in conditions that mimic the experiments described herein.

Additionally, the Lynx MCA was set to take 12 consecutive 30-second measurements without peak summing. This was done to provide maximum flexibility in capturing different temporal regions to provide maximum peak counts for optimal statistics. Post processing of the 12 spectra per measurement will be discussed in the Analysis of Delayed Gamma Spectra portion of this report.

3.3 SAMPLE PREPARATION

Table 3 lists the standards used in all of the following experiments. Each began with an ICP-MS isotopically certified standard diluted in 5% HNO_3 to the specified concentration using solution weights. These fissile content of these standards were later verified with delayed neutron counting methods commonly practiced in the HFIR-NAA facility [3]. Since these samples are thoroughly dissolved in an acid solution, aliquots were added to polythene inserts by using a standard micro-liter scale pipette. In order to maintain the highest accuracy in measurement, inserts were weighed with a mass balance sensitive to 10^{-4} g which was tared from the gross weight, measured immediately after aliquoting the solution to the insert. After this, samples were placed in a drying oven overnight in order to evaporate all of the acid solution from within the insert. Following this, inserts were placed within a high density polyethylene rabbit (a right cylinder with 1.5 cm^3 of internal volume and wall thickness of less than 2 mm), which had the lid heat-sealed using a soldering iron.

Table 3: Standard Solutions used in Experiments

Solution	Elemental Concentration (µg/g)	Fissile Concentration (µg/g)
Natural Uranium	1000	7.200
High Purity ^{233}U	7.851	7.831
Plutonium	1.677	1.300

4. BENCHMARKING THE PERFORMANCE OF THE HFIR DN COUNTER (TASK 1)

The DN counter at the HFIR NAA laboratory was re-configured in 2004 with ^{3}He tubes, from its prior configuration that used BF_3 tubes. Over the years, the noise in the counting system has been increasing, necessitating a higher threshold level setting for the discriminator. It is not clear whether the noise is from signal processing electronics (pickup) or from the ^{3}He tubes themselves. The increased discriminator threshold degrades the sensitivity of the DN counter. One of the tasks for FY 2016 was to optimize the HFIR DN counter by benchmarking its performance to that of a well characterized standard neutron counter and an alternative data acquisition set up. Two separate measurement campaigns were undertaken; (i) DN counting using the ORNL large volume active well coincidence counter (LV-AWCC), with its output connected to a JSR-15 multiplicity shift register and a Canberra LYNX multi-channel scalar (MCS) (ii) pairing each ^{3}He tube from the HFIR DN counter with a PDT (Precision Data Technology) neutron pulse monitoring module[10].

4.1 MEASUREMENTS WITH LV-AWCC

The idea was to irradiate a sample containing a single species of fissile isotope at a known concentration, manually transfer the sample after it is received from the pneumatic tube into the cavity of the LV-AWCC (Figure 7) and determine the total delayed neutron count rate using a Canberra JSR-15 multiplicity shift register module or a LYNX in the MCS mode. Both counting chains are accepted by the IAEA. Since the LV-AWCC has a completely different set of ^{3}He tubes and a signal processing chain, that is free of noise issues, the delayed neutron count rate data from this counter can be trusted. After waiting for a period of time to ensure that all DN activity has decayed away, the same sample would be re-irradiated, transferred to the HFIR DN counter via the pneumatic tube, and counted. After correcting for the efficiencies of the respective counters and for the differences in the time delay before the counting, the delayed neutron count rates from the two neutron counters can be compared. A lower delayed neutron count rate from the HFIR DN counter would be an indication of a degraded sensitivity due to a high discriminator threshold level setting. The benchmarking exercise would also provide an estimate of sensitivity improvement that can be achieved for the HFIR DN counter.

Figure 7. Large Volume Active Well Coincidence Counter

Prior to the measurement campaign using samples, the laboratory space around the DN counter was surveyed for neutron background to select a suitable spot for locating the LV-AWCC. The background measurement was performed with the HFIR at its full power of 85 MW. An ideal location for stationing the LV-AWCC would be one where the count rate neutron background is low (comparable to that registered by the DN counter) and in close proximity to the station where the irradiated sample is retrieved from the pneumatic transfer system. The LV-AWCC was moved around within a radius of about 2 meters from the sample retrieval station and the total neutron background count rate was measured. A Canberra model JSR-15 hand held multiplicity shift register was used to measure the total neutron count rate. The background neutron count rates ranged from 200 counts per second (cps) to 500 cps. The LV-AWCC was shielded with cadmium covers on all sides including the bottom, but the background rates did not reduce much. The source of room return neutrons is thought to be from scattering off the collimators in the beam line in the laboratory below the NAA laboratory. The background recorded by the DN counter is approximately 15 cps. It is low because of the four inches of borated polyethylene shielding that surrounds the ^{3}He tubes. Also, the DN counter assembly is physically located at a height of 12-15 feet above the floor of the NAA lab and this reduces the impact of the scattered neutrons from the beam line below the floor. The LV-AWCC on the other hand, was located directly on the laboratory floor and was susceptible to a much greater interference from scattered neutrons below the floor. The DN count rate from a typical sample (100 ng of ^{235}U) was about 1000 cps which is only about a factor of 2 or 3 greater than the background rate recorded by the LV-AWCC.

For the LV-AWCC background to reduce to a level comparable to that recorded by the DN counter, the LV-AWCC was moved to an adjacent counting room, about 20 feet away from the sample station. Moving the LV-AWCC father away from the sample station would increase the time delay to manually transfer the irradiated sample to the counter.

To evaluate the logistics of the measurement using the LV-AWCC, trial irradiations were performed using evaporated solution samples of ^{235}U and ^{233}U. Samples were irradiated for 60 seconds in PT-2, transferred from the reactor to the NAA laboratory via the pneumatic tube, and then manually transferred to the LV-AWCC. The time delay from the end of irradiation to the beginning of counting in the LV-

AWCC was 30 seconds approximately. A 30 second decay time is longer than the half-life of all but the longest lived delay neutron precursor group (Table 2). The resulting data would consist of counts from delayed neutron precursor groups 1 and 2 primarily and perhaps some contribution from group 3. All of the shorter lived groups would have decayed away significantly. So, a decay time of 30 seconds (which is a result of locating the LV-AWCC 20 feet away from the sample retrieval station) is unacceptably long. By comparison, the decay time for samples counted in the HFIR DN counter is approximately 3 seconds. The delayed neutron decay profile measured by the two counters would be different. So, it was concluded that a proper benchmarking cannot be carried out using the LV-AWCC unless the decay time can be reduced to a value comparable to the decay time for the samples counted in the HFIR DN counter. In nthe reactor off periods, we can compare the counting ratios of standard reference sources such as ^{252}Cf, Am/Li, and Am/Be. This would help benchmark MCNP simulations to be performed in FY2017.

4.2 MEASUREMENTS WITH PDT NEUTRON PULSE MONITORING MODULES

The PDT neutron pulse monitoring modules (Figure 8) offer an attractive alternative to the signal processing chain currently used with the HFIR DN counter.

Figure 8. PDT Neutron Pulse Monitoring Module – Model 20A

For the purposes of testing, the 18 ^{3}He detectors from the DN counter and each ^{3}He detector was paired with a PDT module. The PDT module was connected directly to the ^{3}He tube (Figure 9). The PDT-20A module has a built in high voltage generator that can be adjusted in the 0 – 2200 V range.

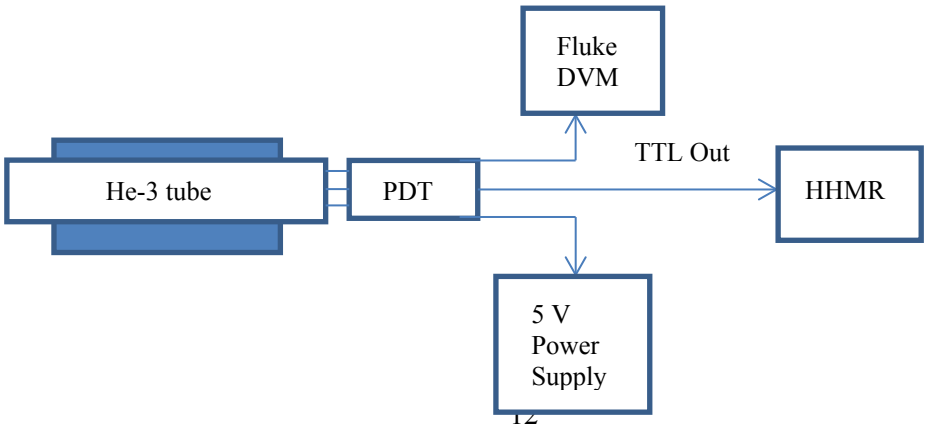

Figure 9. Schematic drawing of the set up for testing ^{3}He tube with PDT module

The PDT based approach has merit because it eliminates the use of long cables that run between the ^{3}He detector and the signal processing chain, potentially eliminating noise interference from the cables. Each PDT module consists of a precision wide band charge sensitive pre-amplifier, an amplifier, wave shaping and discriminator circuits. The goal was to set the amplifier gain in a consistent manner, measure the high voltage plateau of each ^{3}He detector, and set the high voltage at an optimal value. A twelve turn trim pot is available to finely tune the amplifier sensitivity to the desired level.

Each ^{3}He tube being tested was inserted into a block of high density polyethylene moderator. An Am-Li neutron source was placed adjacent to the moderator block. A Fluke digital voltmeter (DVM) was used to monitor the high voltage setting. A Voltec DC power supply was used to provide +5 V power to the amplifier and discriminator circuits. The TTL output from the PDT was input to a handheld multiplicity shift register (HHMR) for counting the neutron events. Figure 9 shows the instrument interconnect diagram. The detectors and sources were set up as depicted in Figure 10 with the Am-Li source on the located between the polyethylene blocks. The detector tube under test was located in position 2. An unused tube was kept in position 4 for the duration of the test to stabilize the spacer block stack. While testing for gamma response, mixed gamma rod sources with ^{241}Am, ^{133}Ba, ^{137}Cs, and ^{60}Co were placed in position 1. The activity of the rod sources was approximately 100 μCi. The gamma sources were removed while testing with Am-Li neutron source.

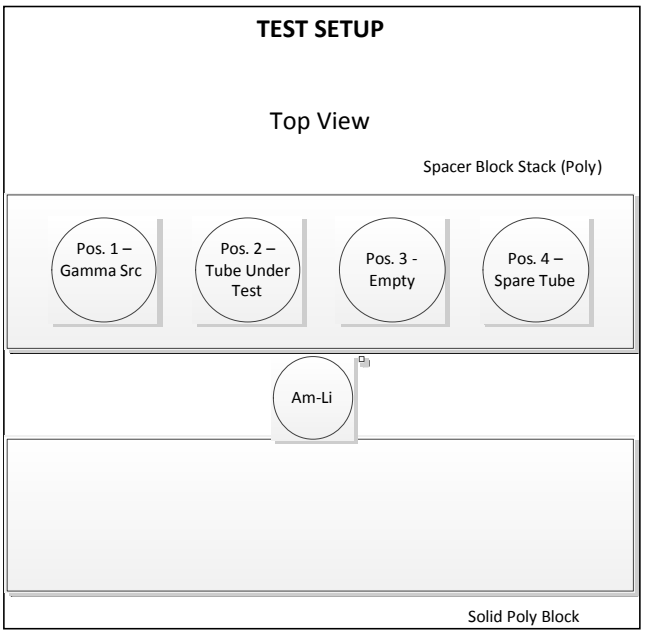

Figure 10. ^{3}He detector test set up

The manufacturer, Precision Data Technology, does not recommend changing the discriminator threshold of PDT-20A modules, originally set at the factory. So, the discriminator thresholds were not changed. The TTL pulse width was adjusted to 50 ns. A twelve turn trim pot is available on the PDT-20A modules to finely tune the amplifier sensitivity to the desired level.

The amplifier sensitivity trim pots of the PDTs were turned to the maximum setting and then backed off five full turns. The Am-Li source was then counted for ten seconds at a range of high voltage settings beginning at 1200 V and ending at 1900 V. Out of the 18 ^{3}He + PDT pairs that were tested, 3 pairs did not work, (i.e.) no neutron counts were registered. It was confirmed that the problem was with the 3 PDT modules and not the ^{3}He tubes. The plots of counts as a function of HV bias are shown in Figure 11.

In an effort to fully populate the DN counter, we tested an additional 24 PDT modules on-hand (returned from the spectroscopy portal monitor program as 'good'.) Allof the units were faulty.

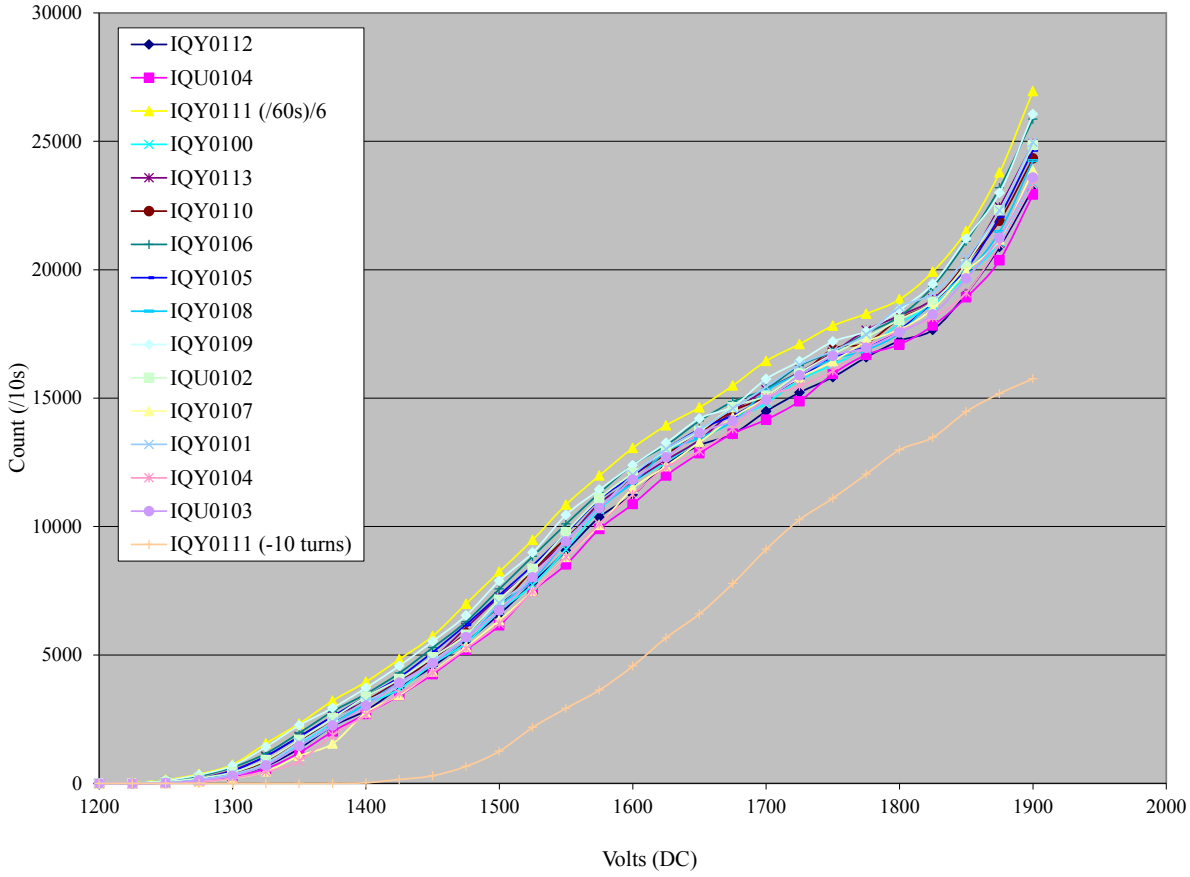

Figure 11. Counting profiles of ^{3}He + PDT-20A pairs

The legend of the plots represent the serial number of the Dextray ^{3}He detectors that generated neutron counts when paired with a PDT-20A module. The amplifier trim pot of one of the assemblies (IQY0111) was turned back ten full turns to determine the effect on the sensitivity. The counts registered were smaller by 80% to 50% in the range between 1500 V and 1650 V, respectively. The shape of the counting profile did not change much, while the sensitivity of the instrument to register counts above the discriminator threshold diminished. The trim pot was then reset and backed off five turns. A "plateau" was recorded using a count time of 60 seconds to determine if an improved precision would be helpful. The counting profile of ^{3}He detector serial # IQY0111 remained similar to that from the other ^{3}He+PDT pairs.

The counting profiles shown in Figure 10 do not look like ^{3}He proportional counter plateau that we are familiar with . An optimal high voltage cannot be selected based on these counting profiles. The best that

one could do is to select a HV at the middle of the range from 1400 volts to 1800 volts. It is possible that the shaping time of the amplifier in the PDT is not a good choice for the Dextray ^{3}He tubes.

The manufacturer, Precision Data Technology is being contacted for advise regarding the compatibility of their modules with the Dextray ^{3}He tubes. A long term approach to improve the HFIR DN counter would be to replace the Dextray tubes with ^{3}He tubes from Reuter-Stokes that are traditionally of a high quality and use proven electronics such as the Amptek boards for signal processing. This would be an investment with long-term benefits.

4.3 PERFORMANCE VERIFICATION OF THE HFIR DELAYED NEUTRON COUNTER (TASK 1)

An extensive irradiation campaign, consisting of 22 samples, was performed in February 2016 to investigate the count rate variation as a function of irradiation time and to confirm linearity of response of the DN counter as a function of the fissile material mass. The samples consisted of natural uranium, plutonium, and ^{233}U. Additionally, there were two samples that were mixtures of U and Pu. The sample characteristics are given in Table 4.

Table 4. Delayed neutron measurement campaign

Sample Description	Mass (ng)	Irradiation time (s)	Wait time (s)	Count time (s)	Counts/ng
Dilute Au, Mn flux monitor foils	N/A	30	N/A	30	N/A
Cellulose swipe blank (J-swipe)	N/A	30	3.0	800	N/A
Nat. U on IAEA J-swipe	155.1	180	3.0	800	1283.5
Nat. U evaporated solution	153.3	180	3.0	800	2032.1
Nat. U evaporated solution	153.3	180	3.0	800	2052.1
^{239}Pu mixed Pu evaporated solution	135.2	180	3.0	800	1553.4
^{233}U 99+% evaporated solution	163.7	180	3.0	800	1409.9
^{233}U 99+% evaporated solution	165.1	180	3.0	800	1277.0
^{233}U linearity std evaporated solution	75.96	180	3.0	800	1351.6
^{233}U linearity std evaporated solution	39.9	180	3.0	800	1309.3
Nat. U/Pu mixture	TBD	180	3.0	800	TBD
Empty container blank	N/A	180	3.0	800	N/A
Nat. U linearity std evaporated solutionn	71.54	180	3.0	800	2068.8
Nat. U linearity std evaporated solution	37.23	180	3.0	800	2063.1
Nat. U evaporated solution	151.84	180	3.0	800	2102.7
^{233}U 99+% evaporated solution	164.451	180	3.0	800	1336.7
Nat. U evaporated solution	153.3	180	3.0	800	2058.5
Nat. U evaporated solution	154.03	180	3.0	800	2075.2
Nat. U evaporated solution	153.3	240	3.0	800	2197.4
Nat. U evaporated solution	155.49	120	3.0	800	1973.1

Table 4. Delayed neutron measurement campaign

Sample Description	Mass (ng)	Irradiation time (s)	Wait time (s)	Count time (s)	Counts/ng
Nat. U evaporated solution	154.76	60	3.0	800	1606.3
Nat. U evaporated solution	154.76	30	3.0	800	1132.5

For confirming the detection limits of the DNAA method, a well-known blank cellulose swipe sample (J-swipe) was also irradiated. It is noted that this was the first time that DNAA had been performed on ^{233}U samples at the HFIR NAA laboratory.

The DN counter data were acquired using a Canberra LYNX DSP in the multi-channel scaling mode in 0.1 second time bins. After the end of irradiation, the earliest time when the count can be started is dictated by the time taken by the rabbit to travel from the reactor to the DN counter. This time, known as the "transfer" time, varies between 1.7 and 2.5 s. A time window with a minimum time of 3.0 s and a maximum of 800 seconds was set up, and the counts from delayed neutrons were summed.

4.3.1 Linearity of DN Counter Response for ^{235}U and ^{233}U

Linearity of response of the DN counter as a function of fissile isotope mass was verified for ^{235}U and ^{233}U (Figures 12a and 12b). The neutron flux normalization (a repeatable process) was performed by foil activation, so that all data could be inter-compared. Repetitions also indicate statistical quality.

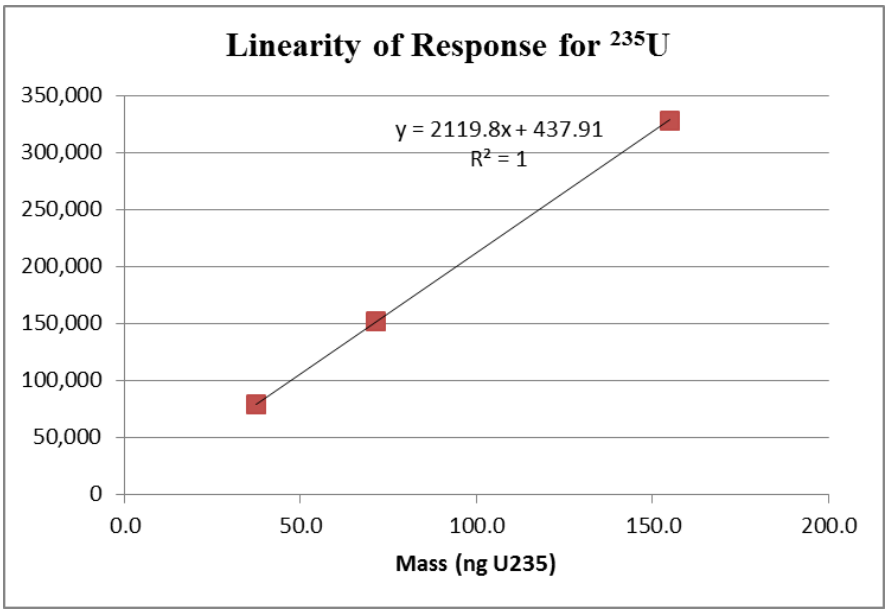

Figure 12a. Linearity of DN Response as a function of ^{235}U mass

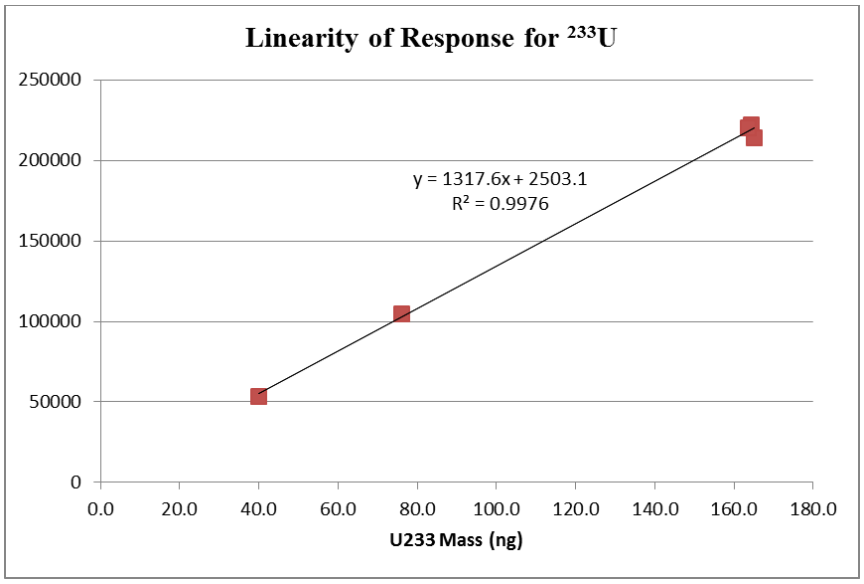

Figure 12b. Linearity of DN Response as a function of ^{233}U mass

Data for ^{235}U indicate excellent linearity. In the case of ^{233}U data, the R^2 statistic is still close to unity, but the larger Y-intercept is worrisome. Clearly, this warrants further investigation and more irradiations of ^{233}U.

4.3.2 Estimation of Detection Limits based on the Blank Cellulose Swipe (J-Swipe)

The cellulose swipe or the Pre-Inspection Check (PIC) samples received from the IAEA are routinely irradiated in the HFIR PT-1 and PT-2 facilities, and DN counting and analyses are carried out. By way of confirming the low detection limits that are achieved using DNAA, a blank cellulose swipe sample was irradiated for 30 seconds in the PT-2 facility, and counted using the LYNX DSP. The detection limit was estimated for a counting period of 60 seconds, consistent with the procedure used for the IAEA sample irradiations.

The detection limit was estimated based on the Currie method [11]. Following the Currie method, an observed signal, S, must exceed a "critical limit" L_C to yield the decision, "detected". Thus, the probability distribution of possible outcomes, when the true (net) signal is zero, intersects L_C such that the fraction, 1 - α, corresponds to the (correct) decision, "not detected". α is the acceptable level of error in deciding that a true signal was detected when it is not present. Mathematically, L_C is expressed by equation (5).

$$L_C = k_\alpha \sigma_0 \qquad (5)$$

In equation (5), k_α is the abscissa of the normal (Gaussian) distribution corresponding to the probability (1-α), and σ_0 is the standard deviation that characterizes the probability distribution of possible outcomes of net signal whose true mean is zero ($\mu_S = 0$).

Once L_C has been established following an experimental observation, an *a priori* detection limit is estimated based on: (i) L_C, (ii) an acceptable level of error β for failing to decide that a signal was present when it was indeed present, and (iii) the standard deviation σ_D that characterizes the probability distribution of possible outcomes of net signal whose true mean is L_D ($\mu_S = L_D$). L_D is defined so that the probability distribution of possible outcomes (when $\mu_S = L_D$) intersects L_C such that the fraction, 1 - β,

will correspond to the (correct) decision, "detected". Equation (6) illustrates the relationship between L_C and L_D.

$$L_D = L_C + k_\beta \sigma_\beta \quad (6)$$

Setting the acceptable level of errors α and β to be the same ($k_\alpha = k_\beta = k$) , and assuming that the standard deviations σ_0 and σ_D are approximately equal, equation (6) can written as follows after substituting for L_C from equation (6).

$$L_D = 2k\sigma \quad (7)$$

The standard deviation of the net signal is derived from:

$$\sigma_S^2 = \sigma_{S+B}^2 + \sigma_B^2 \quad (8)$$

σ^2_{S+B} is the variance in the gross count, and σ^2_B is the variance in the blank counts. If the standard deviation is approximately independent of the signal level, then, equation (8) can be written as follows.

$$\sigma_S^2 = \sigma_{S+B}^2 + \sigma_B^2 = 2\sigma_B^2 \quad (9)$$

Assuming that a misclassification error of 5% are acceptable for α and β , and that the random errors are normally-distributed, the constant k, takes on the value, 1.645. The detection limit at the 95% confidence level is given by equation (10).

$$L_D \approx 3.29 * \sqrt{2\sigma_B^2} \approx 4.65 * \sigma_B \quad (10)$$

Based on the above discussion, the DNAA detection limit was estimated using the counts from the blank cellulose swipe. The results are given in Table 5. The detection limit is converted to mass units using the slope (counts per unit mass) of the linearity plots shown in figures 12a and 12b. We intentionally give more decimal places than are justified to avoid rounding error.

Table 5. DNAA Detection Limits based on blank cellulose swipe samples

Fissile Isotope	Counts from Blank Swipe	Uncertainty in Blank swipe counts	Detection Limit L_D (95% confidence) (counts)	Counts to Mass conversion (counts/picogram)	Detection Limit L_D (95% confidence) (picograms)
^{235}U	105	10.3	47.9	2.1198	22.6
^{233}U	105	10.3	47.9	1.3176	36.4

4.3.3 Delayed Neutron Decay Profiles for Uranium and Plutonium Isotopes

To verify the consistency of the observed neutron count data with the eight-group representation of the precursors, the data was fit using linear combination of eight exponentials as shown in equation (11).

$$C = I_0 \sum_{i=1}^{8} \beta_i \left(1 - e^{-\lambda_i t_{irr}}\right) e^{-\lambda_i t_{dly}} \left(1 - e^{-\lambda_i t_{cnt}}\right), \ counts \quad (11)$$

Equation (11) is similar in form to equation (1) with parameters such as the sample mass, reaction cross section, magnitude of neutron flux and, atomic mass, Avogadro's number and efficiency all combined

into a normalization factor I_0. The best fit was obtained by varying the factor I_0, and the time t_0 that marked the beginning of the delayed neutron decay time after the end of irradiation. Example results are shown respectively in Figures 13a and 13b for ^{233}U and ^{235}U.

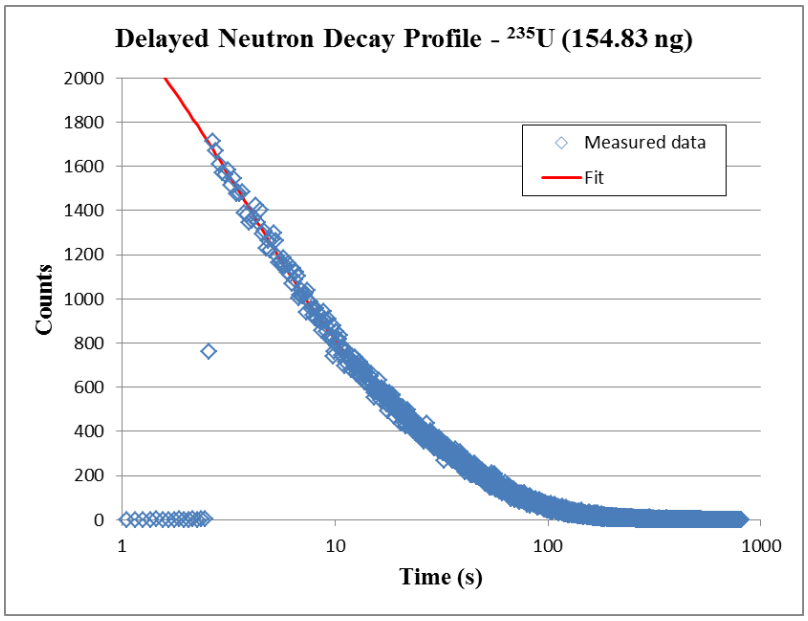

Figure 13a. Delayed neutron decay profile for ^{235}U (154.83 ng)

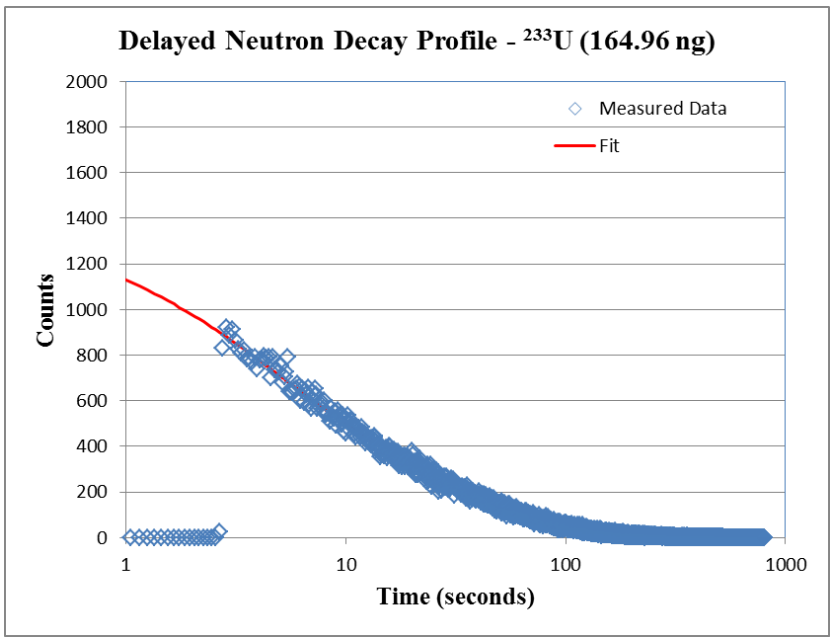

Figure 13b. Delayed neutron decay profile for ^{233}U (164.96 ng)

The reduced chi-squared values were 0.994 and 1.063, respectively, for the ^{235}U and ^{233}U data respectively, thus indicating an excellent fit. Example results are also shown for a ^{239}Pu sample of mass 135 ng (Figure 14a) and a U-Pu mixture of unknown U and Pu masses (Figure 14b).

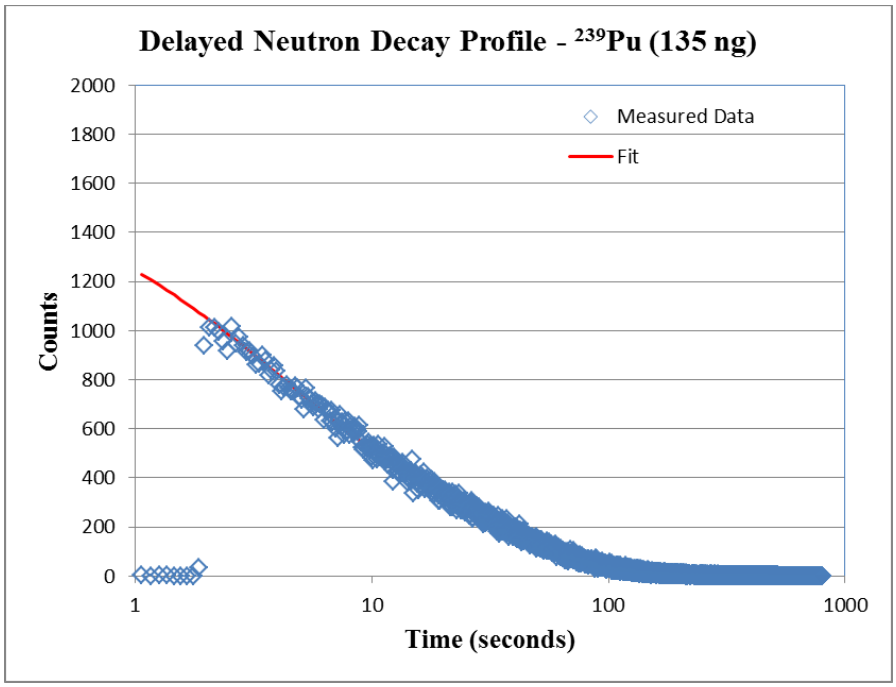

Figure 14a. Delayed neutron decay profile for ^{239}Pu (135 ng)

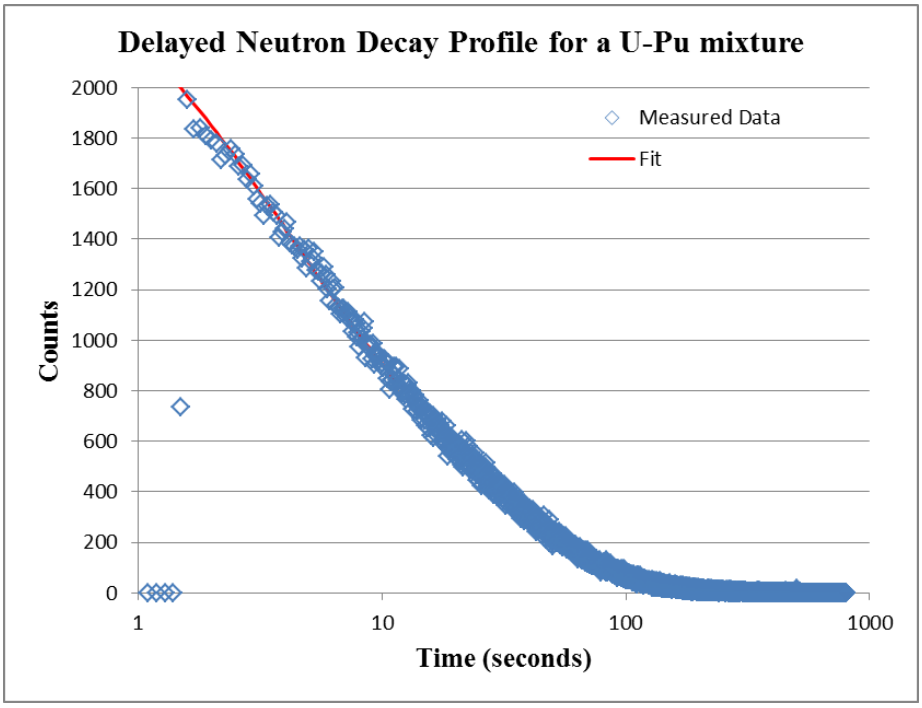

Figure 14b. Delayed neutron decay profile for a U-Pu mixture of unknown mass

For the fit to the data from the ^{239}Pu sample, a reduced chi-squared value of 1.107 was obtained, which is also considered excellent.

The U-Pu sample will consist of delayed neutrons from uranium and plutonium isotopes. The data fit shown in Figure 14b was performed using the DN yields from ^{235}U. A reduced chi-squared value of 1.042 was obtained, indicating a very good fit. Next, the same data was fit using the DN yields from ^{239}Pu, an

equally good fit was accomplished with a reduced chi-squared value of 1.076. Thus, the DN decay curves from U and Pu isotopes are, for practical purposes, indistinguishable. For a sample with an unknown mixture of $^{235}U + ^{239}Pu$, the data could have been obtained with a ^{239}Pu fraction anywhere from 0 to a 100% of the mixture, and the delayed neutron data would not be able to flag it based on a fit to the decay profile. Delayed gamma results will certainly be needed to partition the mass fraction corresponding to ^{235}U and ^{239}Pu.

The delayed neutron decay data from all of the samples irradiated and counted in the February 2016 measurement campaign were fit using the eight exponential functional form. The plots are included in Appendix A. the function fit the decay profiles very well. Of the fits performed on data sets from 18 different samples, the worst reduced chi-squared value obtained was 1.180 and it was for a ^{233}U sample with a mass of 39.9381 ng (Figure A-13 in Appendix A). A fit with a reduced chi-squared of 1.18 is an excellent fit by any standards. It must be noted that these data were acquired using a LYNX signal processor operated in a multi-channel scaling mode. Using the LYNX enabled the acquisition of DN data as a function of time, and to confirm the quality of data by fitting to a physics based exponential functional form.

5. DELAYED GAMMA MEASUREMENTS AND ANALYSIS (TASK 3)

A couple of trial irradiation campaigns were performed to optimize parameters such as irradiation times, count rates, dead times, and the gamma lines from fission products. About 60% of the fission product candidates had half-lives less than 5 minutes, and approximately 40% of the lines had half-lives less than 1 minute. In order to get a high signal to continuum ratio and a good count rate from the short-lived fission products, it is necessary to minimize the time delay between the end of irradiation and the beginning of the sample count on the HPGe detector system. Attempts were made initially to position the gamma detector in closely proximity to a valve underneath the DN counter where the rabbit could be held in place by air currents. The idea was to count the delayed gamma emissions from the sample with minimal delay (less than 10 seconds). And at the end of the gamma counting, the rabbit would drop down into a storage vault (or a "dump tank"). However, the mechanism to hold the rabbit in place at the location of the valve did not work as expected, and the rabbit fell directly into the dump tank before it could be counted using the gamma detector. So, the only available option, one that did not involve an extensive modification of lead shielding around the DN counter, was to bring the rabbit back to a fume hood after the irradiation was completed, and manually transfer the sample into position for gamma spectroscopy.

An extensive irradiation campaign was conducted in August 2016 to test the delayed gamma method. Each sample, contained in a rabbit, was irradiated individually in the well thermalized HFIR PT-2 irradiation facility. At the end of each irradiation, the sample was brought to a fume hood for gamma spectroscopy. Due to sample transfer times between the reactor and fume hood, samples were measured at approximately 19 seconds of decay. The sample was positioned inside of the fume hood at 32.5 cm away from the HPGe detector endcap. Tables 6 and 7 show the single element and binary mixture sample names, fissile material, and fissile mass irradiated in the HFIR-NAA PT-2 facility.

Table 6: Single Element Samples

Sample Name	Fissile Material	Fissile Mass
J29	^{235}U	49.68
J30	^{235}U	102.24
J31	^{235}U	150.48
J32	^{235}U	203.04

J33	^{235}U	252.72
J34	^{233}U	46.99
J35	^{233}U	94.76
J36	^{233}U	141.74
J37	^{233}U	189.51
J38	^{233}U	237.28
J49	^{239}Pu	40.04
J50	^{239}Pu	85.15
J51	^{239}Pu	172.92
J52	^{239}Pu	260.69
J53	^{239}Pu	301.30

Table 7: Binary Mixture Samples

Sample Name	Fissile Materials	Ratio	Total Fissile Mass
J39 J44	$^{235}U/^{233}U$	0.293	162.02
J40 J45	$^{235}U/^{233}U$	0.566	159.40
J41 J46	$^{235}U/^{233}U$	1.021	158.23
J42 J47	$^{235}U/^{233}U$	1.487	157.75
J43 J48	$^{235}U/^{233}U$	3.021	154.29
J54 J59	$^{239}Pu/^{235}U$	0.117	127.87
J55 J60	$^{239}Pu/^{235}U$	0.387	141.76
J56 J61	$^{239}Pu/^{235}U$	1.177	159.90
J57 J62	$^{239}Pu/^{235}U$	2.188	169.87
J58 J63	$^{239}Pu/^{235}U$	4.003	180.10

Post-processing of gamma spectra was conducted using PeakEasy software [12]. PeakEasy was developed by Los Alamos National Laboratory and Sandia National Laboratories in 2006 for rapid nuclide identification and analysis of gamma-ray spectra. PeakEasy was used in this work due to its high accuracy in producing Gaussian fits to measured isolated photopeaks, spectra summing capabilities, and precise replication of those fits over a batch processing routine.

5.1 FISSION PRODUCT IDENTIFICATION

Prior to running experiments with samples containing fissile materials, rabbits containing empty inserts were irradiated and measured at the HFIR-NAA lab under the same conditions as the following experiments. Figure 15**Figure 15:** Blank Rabbit Spectrum (Summed over 12x30 second measurements) shows the blank rabbit spectrum summed over the 12 30-second measurement intervals as described earlier. The activation products identified after an empty rabbit irradiation in PT-2 were: ^{56}Mn, ^{28}Al, ^{38}Cl, ^{41}Ar, and ^{51}Cr. The ^{56}Mn, ^{28}Al, and ^{38}Cl are activation products made from impurities within the high-density polyethylene (HDP) matrix, while ^{41}Ar is created from activation of elemental Argon in air trapped within the rabbit, and ^{51}Cr is created from activated Chromium acquired from the stainless steel pneumatic tube. These activation products were identified through verification of major and minor photopeaks using the NuDat nuclear database [12]. As can be seen in 8, the major photopeaks of these activation products do not give interferences to the short-lived fission product photopeaks used in this analysis.

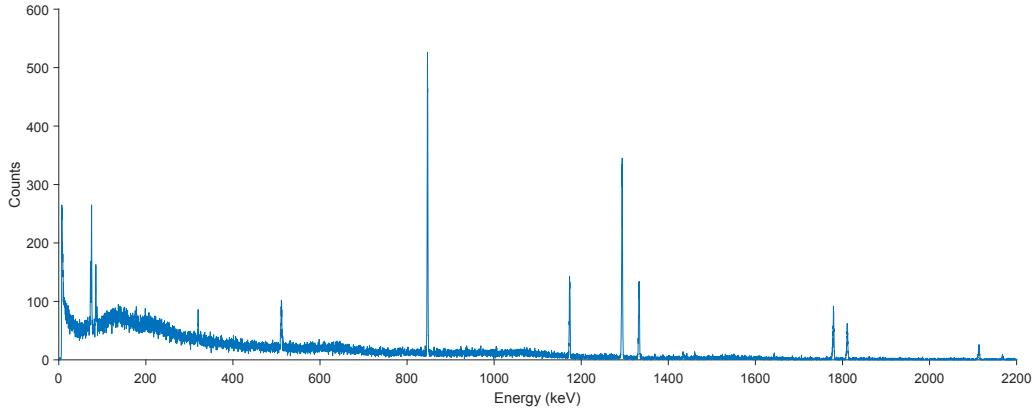

Figure 15: Blank Rabbit Spectrum (Summed over 12x30 second measurements)

Table 8: Photopeaks Identified in Blank Rabbit Gamma Spectrum

Energy (keV)	Isotope
2168	Cl-38
2113	Mn-56
1810	Mn-56
1779	Al-28
1642	Cl-38
1332	Co-60
1293	Ar-41
1173	Co-60
846	Mn-56
320	Cr-51
75	Pb (k,α)

Following the blank rabbit gamma spectrum measurements, fission product photopeaks were identified from Natural Uranium, ^{233}U, and Plutonium samples (example spectra seen in Figures 16–18). Peak identification for a spectrum containing short-lived fission products can be a significant challenge. Often, only a small fraction of the photopeaks emitted from a given fission product are uninterfered in the spectrum, making it difficult to rely on confirming photopeaks from NuDat [13]. To address this issue, ORIGEN [6] simulations were run with the irradiation and decay conditions seen in the HFIR-NAA laboratory in order to isolate the fission product photopeaks that will be good candidates for testing the methodology. The basic fission product yield data is not always of high accuracy but it is the best complete approach we have and is adequate for scoping studies prior to experiment.

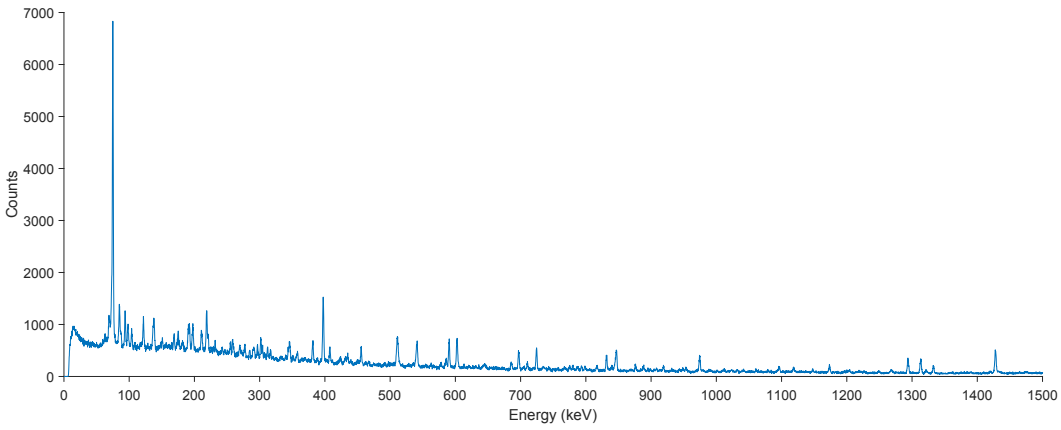

Figure 16: Natural uranium gamma spectrum (J33 summed over 12x30 second intervals)

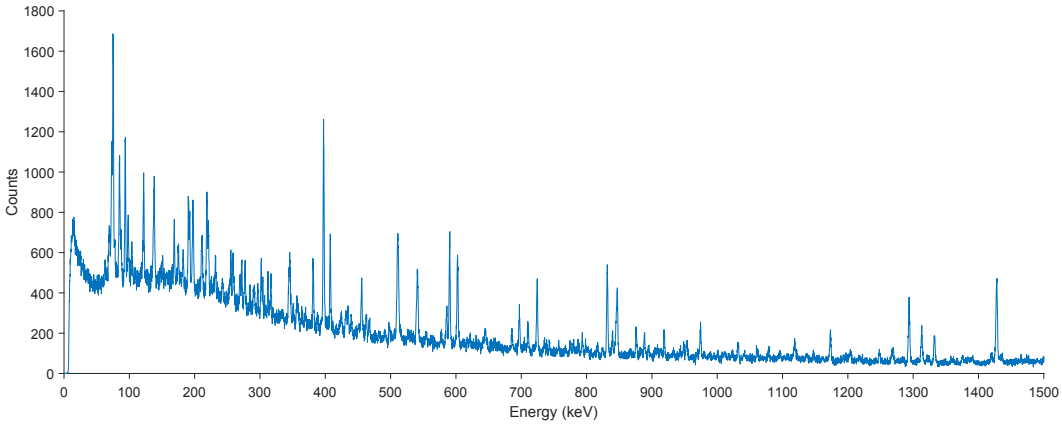

Figure 17: ^{233}U gamma spectrum (J38 summed over 12x30 second intervals)

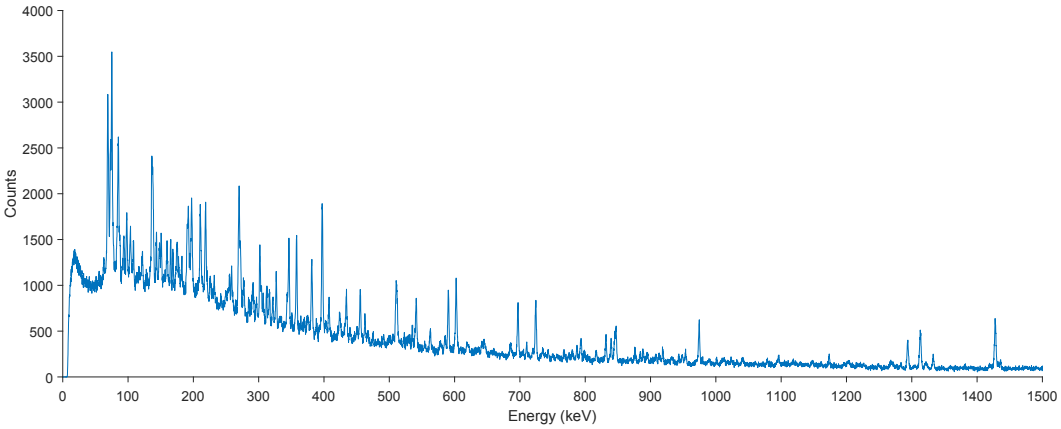

Figure 18: Plutonium gamma spectrum (J53 summed over 12x30 second intervals)

Table 9 lists the fission products identified from conducting ORIGEN runs and comparing with nuclear data on NuDat. ^{239}U is not a fission product, but was left on this list because it can be a reliable method of quantifying ^{238}U content within a uranium matrix using standard NAA analysis techniques, and it is the most prominent peak in Figure 16. It should be noticed that there is significant variability in the half-lives of the fission products measured; from less than 30 seconds to nearly 20 minutes. Therefore, a peak summing routine was adopted: photopeaks with half-lives of less than 5 minutes were summed for over first 4x30 second measurements and half-lives of greater than 5 minutes were summed for over the last 8x30 second measurements. This summing routine was then combined with a PeakEasy batch process to integrate Regions of Interest (ROIs) around each of the fission product photopeaks listed in Table 9. From this point forward the count rates of each photopeak are used (measured in Counts per Second) for developing photopeak ratios.

Table 9: Fission Product Photopeaks Identified in Irradiated Sample Spectrum

Energy (keV)	Isotope	Half-Life (m)
686	Sr-95	0.398
1119	Kr-90	0.539

270	Tc-106	0.593
541	La-144	0.68
397	La-144	0.68
562	Tc-103	0.903
346	Tc-103	0.903
136	Tc-103	0.903
1313	I-136	0.916
381	I-136	0.916
603	Cs-140	1.062
1427	Sr-94	1.255
725	Ce-145	3.01
974	Sb-132	3.2
697	Sb-132	3.2
832	Rb-90	3.33
455	Xe-137	3.818
434	Rh-108	6
793	Sb-130	6.3
1269	Sr-93	7.43
888	Sr-93	7.43
876	Sr-93	7.43
710	Sr-93	7.43
590	Sr-93	7.43
954	Y-95	10.3
407	Te-133	12.5
358	Tc-104	18.3
919	Y-94	18.7
74.66	U-239	23.45

5.2 CHOOSING PHOTOPEAK RATIOS

As discussed in Beddingfield's (who was the first to propose) [15], an effective means for establishing fissile isotope signatures from fission products is to ratio the high mass fission product photopeaks with low mass counterparts. Therefore, the isotopes were broken into two categories: atomic masses less than 130 and greater than 130. These two groups were used as numerators and denominators when making fission product photopeak count rate ratios. Due to the large number of ratios, known problematic photopeaks were removed from the analysis. These fission products are known to be volatile, or originate from volatile parents, and escape the rabbit at an unknown rate. The fission products removed from this analysis are: Kr-90, I-136, Rb-90, and Xe-137. The entire list of photopeak ratios analyzed is shown in Appendix B.

5.3 LINEARITY STUDY (TASK 3, TASK 4)

A linearity study was conducted to confirm the variation of low mass to high mass fission product ratios as a function of ^{239}Pu concentration using the delayed gamma experiments described earlier in this report. In FY16, the focus was on mixtures of ^{235}U and ^{239}Pu, while ^{233}U is intended to be added in FY17. Figures 19 through 30 show the results of this linearity study for 12 different ratios. These ratios are considered the strongest indicators of the Pu/U mixture concentration due to their high coefficient of

determination to a linear fit (also known as r^2 value). The coefficient of determination is the square of the Pearson sample and linear correlation coefficient (equation 12).

$$r = \frac{n\sum xy - \left(\sum x\right)\left(\sum y\right)}{\sqrt{n\left(\sum x^2\right) - \left(\sum x\right)^2}\sqrt{n\left(\sum y^2\right) - \left(\sum y\right)^2}} \quad (12)$$

In equation (12) x and y are the independent and dependent variables, respectively (although the order of the labels can be switched) and n is the number of (x,y) pairs.

The figures contain uncertainties in both the x and y-directions. Currently, the uncertainties for photopeak ratios represent propagated counting statistics from the DLFC corrected spectrum, likely underrepresenting true uncertainty because the DLFC technique does not preserve Poisson precision.. It is the authors' intent to transition to using uncorrected spectrum, but additional data analysis will be required in FY2017 to complete this task. The uncertainties in the fractional ^{239}Pu concentration (x-axis) are a function of mass uncertainty in the sample preparation itself. Since a 5 figure balance (with smallest measurement at 0.1 grams) was used, the uncertainty for each measurement was valued at 0.2 grams. This uncertainty only becomes apparent in mixtures, since a high degree of confidence can be applied to fissile isotope ratios for a sample only containing Pu or U isotopes. The uncertainties in the photopeak ratios (y-axis) are a function of counting statistics propagated throughout the summing of the spectra and calculating the ratio of two photopeaks.

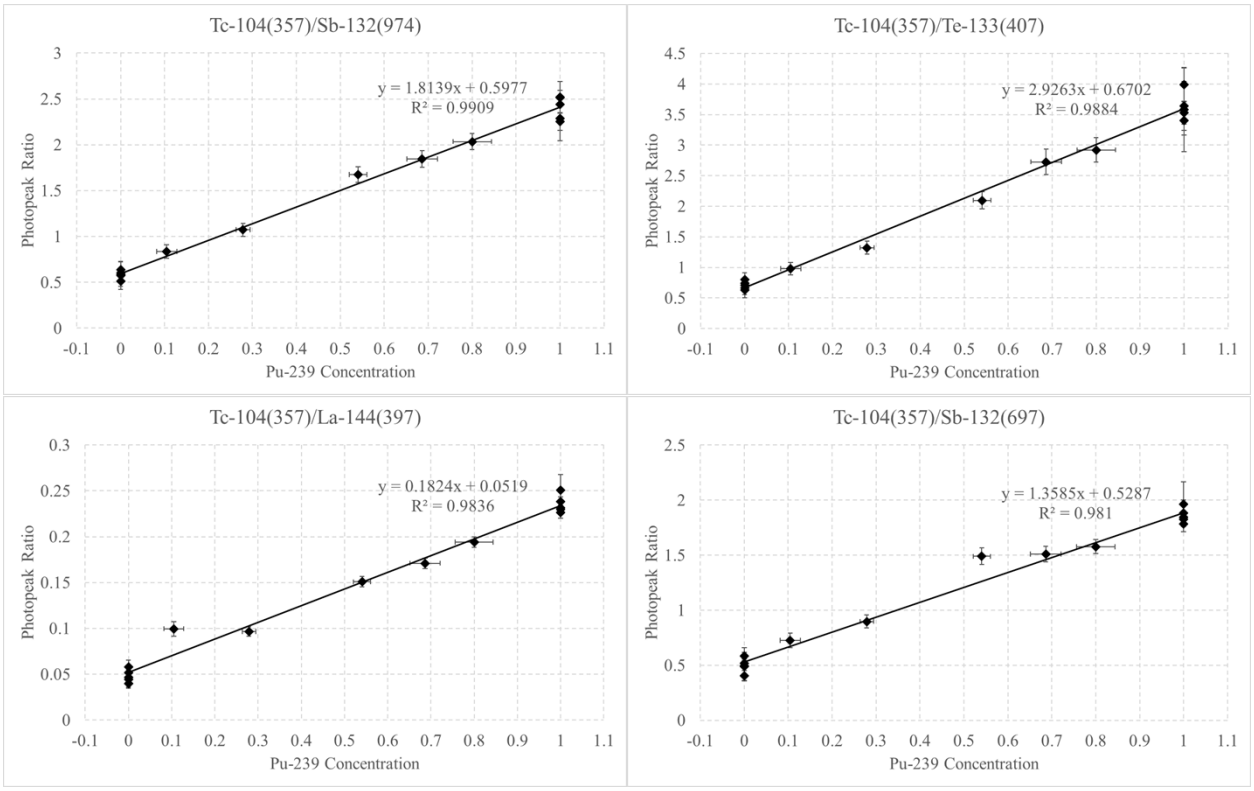

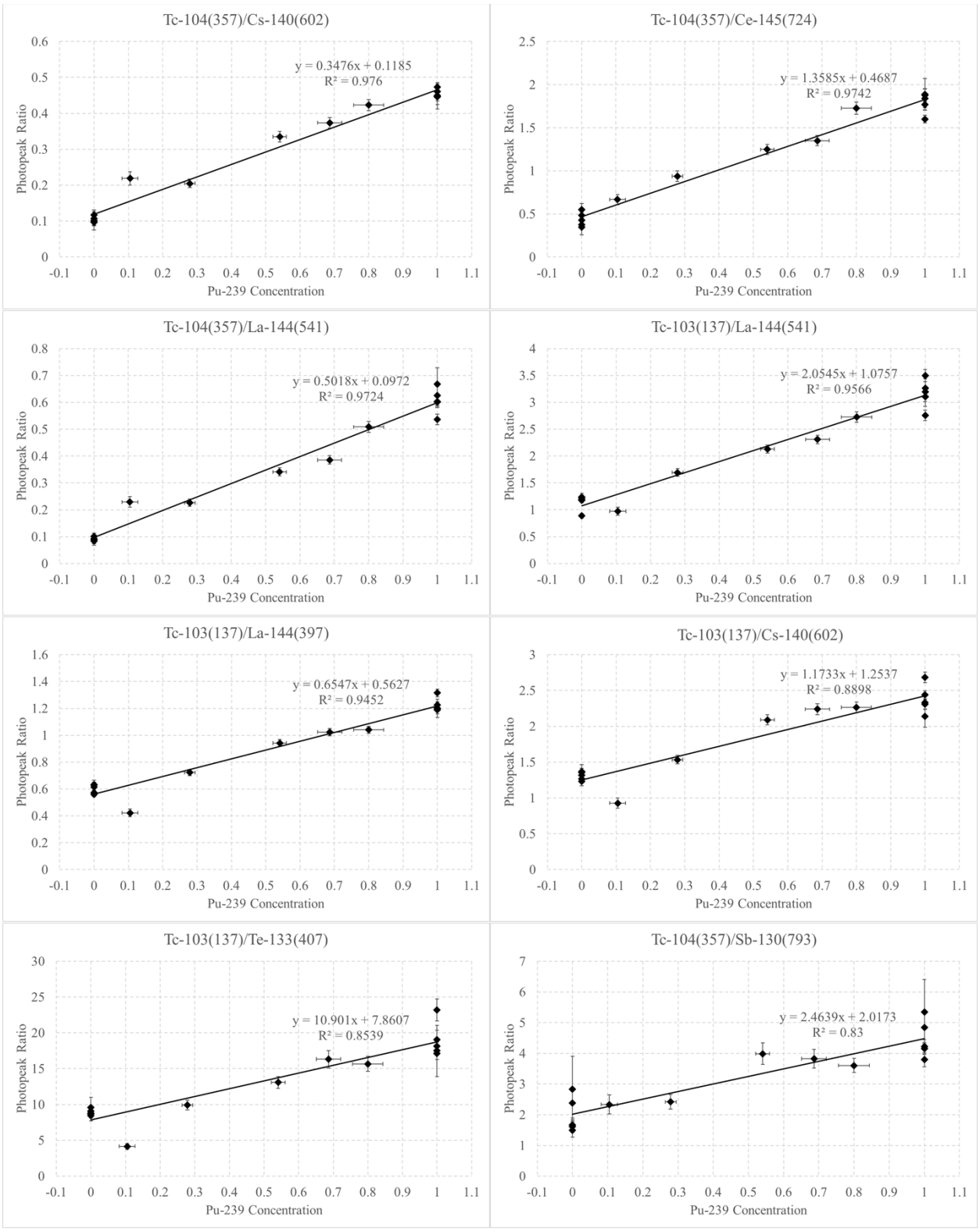

Figures 19–30: Linearity study of 12 different fission product photopeak ratios

Out of the 56 ratios that were considered, only those linear fits with a value of 0.90 for the correlation coefficient r (or $r^2 = 0.81$) were selected. This criterion for the selection of fission product ratios will be further refined based on analyses performed in FY17. Irradiations were performed in September 2016 reactor cycle. The data is being analyzed and the results will be reported in the FY2017 Q2 quarterly report.

Besides confirming linearity, the plots of fission product ratios versus ^{239}Pu fraction (in a ^{235}U+^{239}Pu binary mixture) will also serve as an empirical calibration for a given ratio of low mass to high mass fission product.

6. ANALYTICAL SYSTEM FOR DNDG (TASK 4)

The DNDG method and instrumentation are not meant to be applicable solely at the HFIR facility at ORNL. The methodology and the instrumentation could be made generic to many research reactor facilities around the world. The excellent sensitivities achieved from DNAA at the HFIR are indeed possible because of high thermal fluxes on the order 10^{14} $n.cm^{-2}.s^{-1}$. But there are several research reactors in the world that can deliver thermal fluxes comparable to the HFIR flux. The IAEA website provides information on research reactors worldwide [17]. Out of the worldwide list, a subset of research reactors in North America and Western Europe that can deliver a thermal power of more than 4 MW are listed in Appendix D. Each of the reactors listed in Appendix D could be a candidate for performing DNDG analysis. The magnitude of available thermal flux will dictate the sensitivities that can be achieved.

A DNDG analysis system requires the following infrastructure and instrumentation.

1. A thermal neutron irradiation field that can deliver a flux of 10^{12} $n.cm^{-2}.s^{-1}$ (for achieving a detection limit of approximately 5 ng of ^{235}U equivalent mass)
2. A mechanism to transfer the irradiated sample to a counter, within a 10 second time delay.
3. A thermal neutron counter (made of ^{3}He or BF_3 or boron coated straw detectors embedded in polyethylene) that can detect delayed neutrons. The efficiency of the counter can be in the 20% to 25% range. The tubes can be bought Commercial Off The Shelf (COTS), and the counter can be designed following the ORNL DN counter
4. COTS signal processing components or modules for counting delayed neutrons (e.g. Amptek amplifier and discriminator boards, LYNX DSP used in MCS mode)
5. Gamma spectrometry system with an HPGe detector with a 40% relative efficiency, DSP MCA such as Canberra's LYNX or Ortec's DSPEC, and associated software for data acquisition and peak analysis.
6. Graded lead shielding around the HPGe.
7. Computers

The research reactor facilities (at least the ones in North America and Western Europe) may already have the necessary infrastructure and instrumentation for performing DNDG analysis. The DNDG instrumentation and procedure can be standardized, with minimal customizations depending on facility requirements.

Currently, the data reduction and analysis has been done using excel spreadsheets. Automating the analysis will enhance the usability of the method, and will avoid human errors. As an example of such automation, one of the authors (Justin Knowles) developed a utility to flag the presence of ^{239}Pu in a mixture of ^{235}U+^{239}Pu, leveraging his previous work [5]. The utility uses as inputs the measured low mass to high mass FEP ratios from the unknown sample (binary mixture), calculated values of low mass to

high mass FEP ratios from ^{235}U only and ^{239}Pu only (the Beddingfield approach). The utility called as the "ORNL Safeguards Actinide Concentration Calculator" or ORNL-SACC is described in Appendix C. In FY17, the ORNL-SACC will be adapted to use the empirical calibration data from the DG analysis instead of the calculated FEP ratios.

7. CONCLUSIONS

Work done in Q1 and Q2 of FY16 revealed the challenges involved in trying to configure the ^{3}He detectors from the DN with alternative signal processing modules (the PDT neutron counting modules). A high neutron background at the desired measurement location precluded the use of the LV-AWCC to benchmark the DN counter performance. However, the LYNX DSP was successfully used in the MCS mode to count delayed neutrons. Samples containing single fissile species of ^{235}U, ^{233}U, and ^{239}Pu were irradiated and the DN data was acquired using the LYNX. The DN data was acquired using the LYNX in 0.1 second time bins. Use of the LYNX enabled the DN decay profile to be recorded. The data were fit using an eight exponential function. The excellent quality of the fits revealed that the data acquired using the LYNX was reliable. The DN decay profile showed that it was not possible to distinguish between ^{235}U and ^{239}Pu based on DN data alone. Preliminary results were presented at the 2016 annual meeting of the Institute of Nuclear Materials Management (INMM) [18]. Based on the irradiation of a blank cellulose swipe, the detection limits (at 95% confidence level) for the DNAA of ^{235}U and ^{233}U were established to be 23 picograms and 36 picograms, respectively.

The work done in Q3 qnd Q4 of FY 2016 has demonstrated that the DG analysis can be used to establish ratios of low mass to high mass fission product FEP counts, that are sensitive to the presence of ^{239}Pu in a binary mixture of ^{235}U+^{239}Pu. Fission product candidates suitable for the DNDG work were evaluated, and 12 FEP ratios of low mass to high mass fission products have been identified. Data from irradiations performed in September 2016 are being analyzed to further refine the calibration, and propagation of uncertainties.

8. FUTURE WORK (FY2017)

The scope of work for FY2017 is as follows.

- **Task 1:** Refine the DNDG method.
    - Conclusively establish the Low Mass/High Mass fission product ratios that can be used to apportion the fractions of ^{235}U and ^{239}Pu in a binary mixture. Complete the empirical calibration.
    - Determine the ^{235}U equivalent mass from a mixture of ^{235}U and ^{239}Pu using delayed neutron counting.
    - Combine the results of delayed neutron and delayed gamma analyses to quantify ^{235}U and ^{239}Pu.
- **Task 2:** Establish the figures of merits for the DNDG technique: (i) detection limits (ii) timing regimes (iii) uncertainty quantification (iv) linear response range. These would include tests with swipe samples.

- **Task 3:** Apply the method to the IAEA cellulose swipe samples (Pre-Inspection Check or PIC samples). Draft a procedure for incorporating the new DNDG measurement regime.

- **Task 4:** Design study using MCNP modeling to improve the sensitivity of the delayed neutron counter by re-arranging the He-3 tubes, and possibly adding another ring. Optimize the moderator thickness and tube placement using MCNP in order to achieve the best possible efficiency.

We have indicated hardware and software upgrade potential which is outside of the scope. Detailed flux and irradiation spectrum mapping as well as modeling is needed to better understand the responses from first principles. International collaboration with other NAA facilities would be another productive avenue.

9. ACKNOWLEDGEMENT

The authors would like to thank the United States Department of Energy NA 24 Office of Nonproliferation and Arms Control for funding the research project.

10. REFERENCES

1. D. H. Beddingfield, Identification and Quantification of Pu and U from Fission Product Gamma-Ray Spectra, Ph.D. Thesis, Colorado School of Mines, 1996.
2. S. E. Binney and R. I. Scherpelz, "A review of the delayed fission neutron technique," Nuclear Instruments and Methods in Physics Research, 154, Issue 3, Pages 413-431, 1 September 1978.
3. D. C. Glasgow, I. J. Park, S. M. Hayes, J. S. Shin, J. A. Carter, and J. M. Whitaker, "Fast, Sensitive, and Accurate Fissile Determination for Nuclear Nonproliferation Applications by Neutron Activation Analysis and Delayed Neutron Counting," in Institute of Nuclear Materials Management Annual Meeting, 2004, pp. 1–10.
4. R. Kapsimalis, D. Glasgow, B. Anderson, S. Landsberger, "The simultaneous determination of ^{235}U and ^{239}Pu using delayed neutron activation analysis," J. Radioanal. Nucl. Chem. (2013) 298:1721–1726.
5. J. Knowles, S. Skutnik, D. Glasgow, and R. Kapsimalis, "A Generalized Method for Characterization Of 235U and 239Pu Content Using Short-Lived Fission Product Gamma Spectroscopy," Nucl. Instruments Methods Phys. vol. 1(2016).
6. I. C. Gauld, G. Radulescu, G. Ilas, B. D. Murphy, M. L. Williams, and D. Wiarda, "Isotopic Depletion and Decay Methods and Analysis Capabilities in Scale," Nucl. Technol., vol. 174, pp. 169–195, 2011.
7. G. Rudstam, Ph. Finck, A. Filip, A. D'Angelo, and R. D. McKnight, "Delayed Neutron Data for the Major Actinides," NEA/WPEC-6, 2002.
8. ORTEC, "ICS: Integrated Cryocooling System," 2015.
9. Canberra Industries, "Lynx Digital Signal Analyzer User's Manual," 2008.
10. PDT20A compact neutron monitoring modules, Precision Data Technologies, Inc., www.pdt-inc.com
11. Lloyd A. Currie, "Limits for Qualitative Detection and Quantitative Determination - Application to Radiochemistry", Vol. 40, No. 3, March 1968, pp. 586-593.
12. Los Alamos National Laboratory, "PeakEasy Home Page," 2016. [Online]. Available: https://peakeasy.lanl.gov/.
13. Brookhaven National Laboratory, "National Nuclear Data Center." [Online]. Available: http://www.nndc.bnl.gov/nudat2/.
14. R. E. Marrs, E. B. Norman, J. T. Burke, R. a. Macri, H. a. Shugart, E. Browne, and A. R. Smith, "Fission-product gamma-ray line pairs sensitive to fissile material and neutron energy," *Nucl.*

Instruments Methods Phys. Res. Sect. A Accel. Spectrometers, Detect. Assoc. Equip., vol. 592, no. 3, pp. 463–471, 2008.
15. D. Beddingfield and F. Cecil, “Identification of fissile materials from fission product gamma-ray spectra,” *Nucl. Instruments Methods Phys. Res. Sect. A Accel. Spectrometers, Detect. Assoc. Equip.*, vol. 417, no. 2–3, pp. 405–412, 1998.
16. M. T. Andrews, J. T. Goorley, E. C. Corcoran, and D. G. Kelly, “MCNP6 simulations of gamma line emissions from fission products and their comparisons to plutonium and uranium measurements,” *Prog. Nucl. Energy*, vol. 79, pp. 87–95, 2015.
17. https://nucleus.iaea.org/RRDB/RR/ReactorSearch.aspx
18. S. Croft, R. Venkataraman, R. D. McElroy, S. Cleveland, D. Glasgow, and J. Knowles, "Delayed Neutron and Delayed Gamma Counting To Co-detect and Quantify Trace Quantities of Uranium and Plutonium" Proceedings of the 57th INMM Annual Meeting July 24-28, 2016, Atlanta, GA, USA.

APPENDIX A: DELAYED NEUTRON DECAY PROFILES FOR FISSILE ISOTOPES

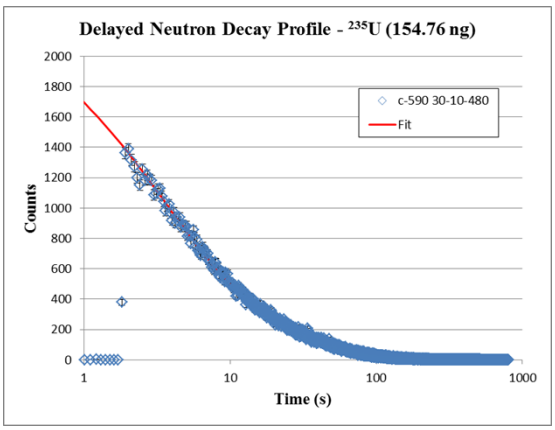

Figure A-1: DN decay profile: ^{235}U Sample 1

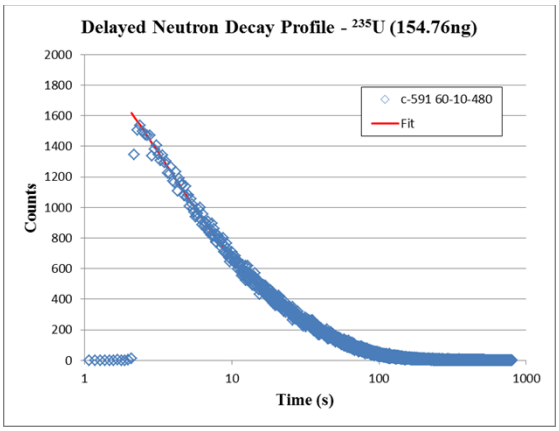

Figure A-2: DN decay profile: ^{235}U Sample 2

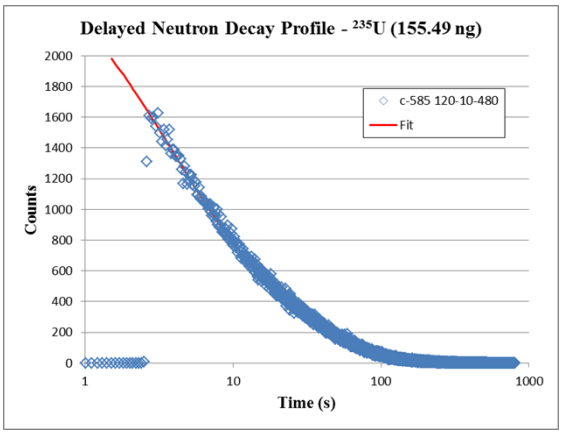

Figure A-3: DN decay profile: ^{235}U Sample 3

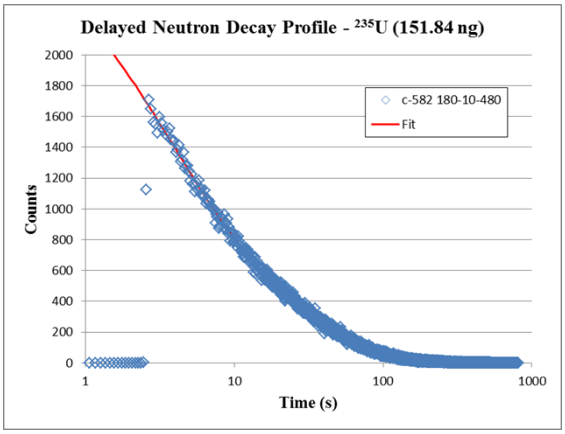

Figure A-4: DN decay profile: ^{235}U Sample 4

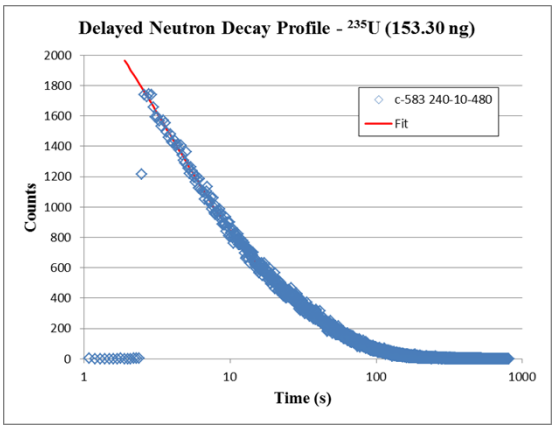

Figure A-5: DN decay profile: ^{235}U Sample 5

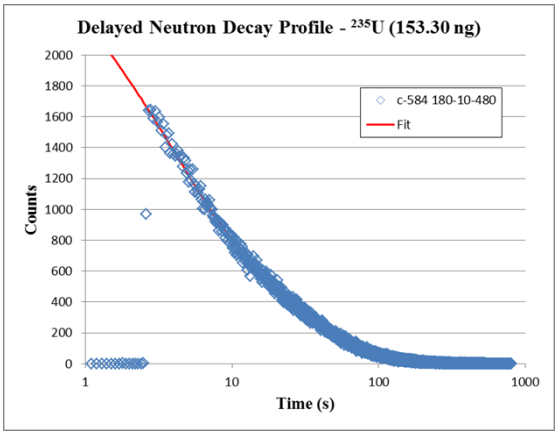

Figure A-6: DN decay profile: ^{235}U Sample 6

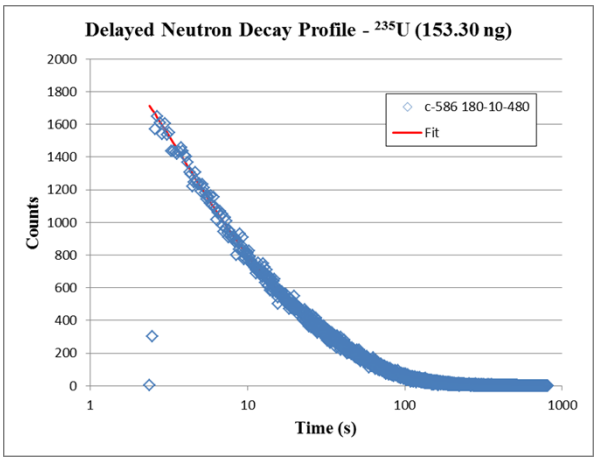

Figure A-7: DN decay profile: ^{235}U Sample 7

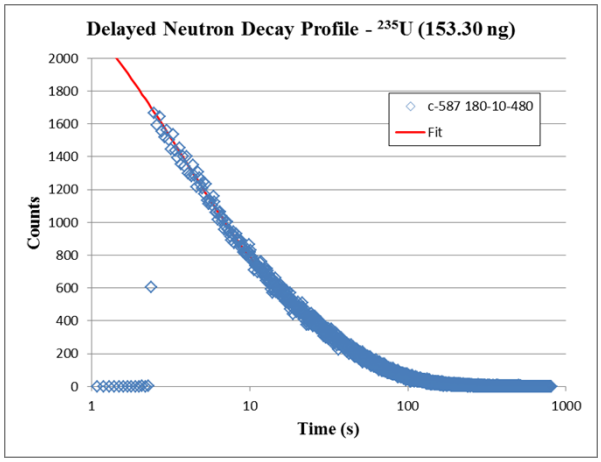

Figure A-8: DN decay profile: ^{235}U Sample 8

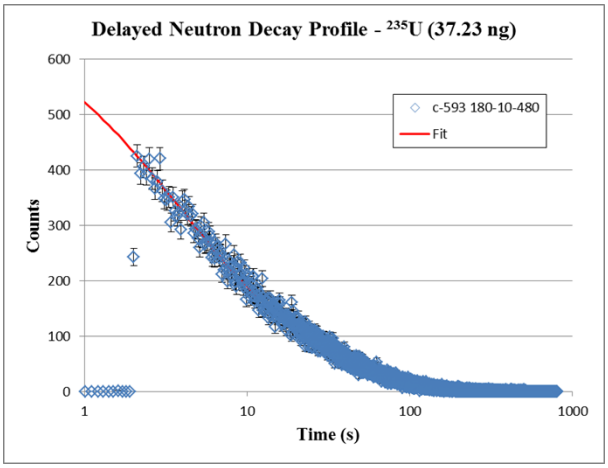

Figure A-9: DN decay profile: ^{235}U Sample 10

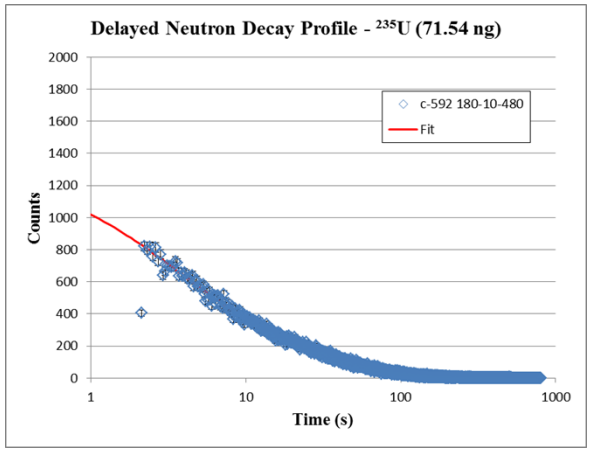

Figure A-10: DN decay profile: ^{235}U Sample 11

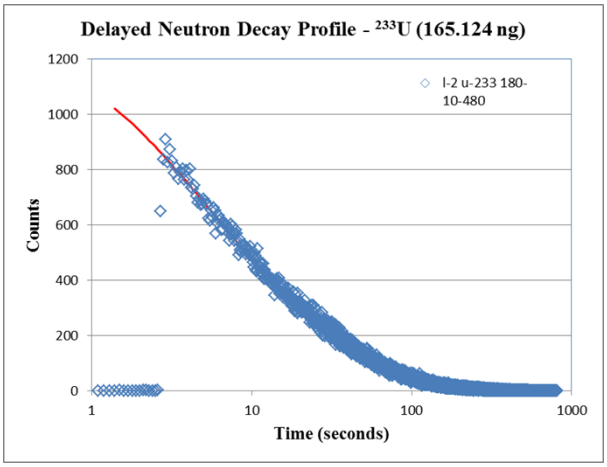

Figure A-11: DN decay profile: ^{233}U Sample 2

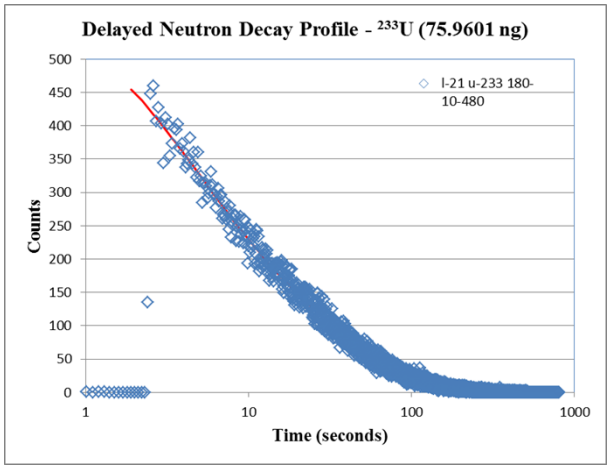

Figure A-12: DN decay profile: ^{233}U Sample 3

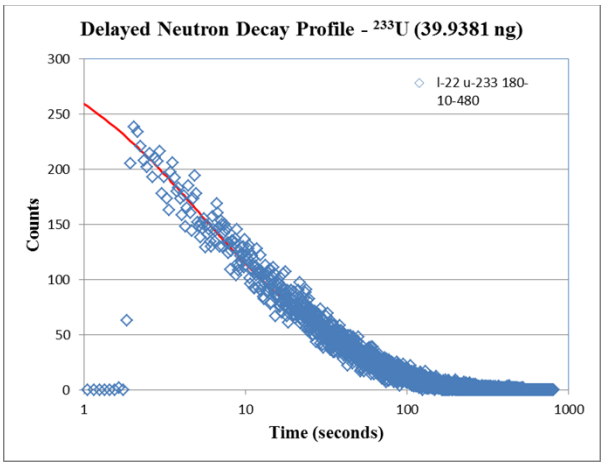

Figure A-13: DN decay profile: ^{233}U Sample 4

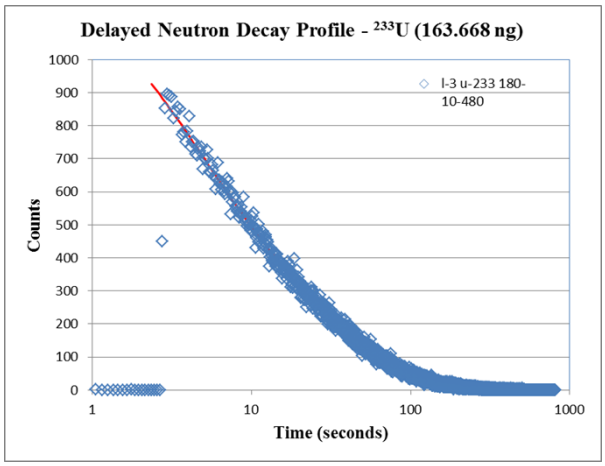

Figure A-14: DN decay profile: ^{233}U Sample 5

APPENDIX B: FULL LIST OF FISSION PRODUCT PHOTOPEAK RATIOS

Low Mass Isotope (kev) (numerator)	High Mass Isotope (kev) (denominator)	Ratio Number	R^2 Statistic
Sr-94 (1428)	Sb-132 (974)	1	0.3678
	Sb-130 (793)	2	0.6691
	Ce-145 (724)	3	0.1663
	Sb-132 (697)	4	0.6402
	Cs-140 (602)	5	0.1229
	La-144 (541)	6	0.4513
	Te-133 (407)	7	0.4603
	La-144 (397)	8	0.0125
Sr-93 (710)	Sb-132 (974)	9	0.7719
	Sb-130 (793)	10	0.5942
	Ce-145 (724)	11	0.7382
	Sb-132 (697)	12	0.8022
	Cs-140 (602)	13	0.5200
	La-144 (541)	14	0.0436
	Te-133 (407)	15	0.1367
	La-144 (397)	16	0.3649
Sr-95 (685)	Sb-132 (974)	17	0.0630
	Sb-130 (793)	18	0.4931
	Ce-145 (724)	19	0.0705
	Sb-132 (697)	20	0.1821
	Cs-140 (602)	21	0.0411
	La-144 (541)	22	0.4341
	Te-133 (407)	23	0.0440
	La-144 (397)	24	0.0036
Sr-93 (590)	Sb-132 (974)	25	0.0550
	Sb-130 (793)	26	0.5623
	Ce-145 (724)	27	0.0579
	Sb-132 (697)	28	0.3211
	Cs-140 (602)	29	0.0136
	La-144 (541)	30	0.3154
	Te-133 (407)	31	0.4097
	La-144 (397)	32	0.0262
Tc-104 (357)	Sb-132 (974)	33	0.9909
	Sb-130 (793)	34	0.8300
	Ce-145 (724)	35	0.9742
	Sb-132 (697)	36	0.9810
	Cs-140 (602)	37	0.9760
	La-144 (541)	38	0.9724
	Te-133 (407)	39	0.9884
	La-144 (397)	40	0.9836
Tc-103 (345)	Sb-132 (974)	41	0.0297
	Sb-130 (793)	42	0.5117
	Ce-145 (724)	43	0.0280
	Sb-132 (697)	44	0.1395
	Cs-140 (602)	45	0.0062
	La-144 (541)	46	0.3803
	Te-133 (407)	47	0.1793
	La-144 (397)	48	0.0299

Tc-103 (137)	Sb-132 (974)	49	0.7947
	Sb-130 (793)	50	0.0001
	Ce-145 (724)	51	0.8104
	Sb-132 (697)	52	0.7472
	Cs-140 (602)	53	0.8898
	La-144 (541)	54	0.9566
	Te-133 (407)	55	0.8539
	La-144 (397)	56	0.9452

Out of the 56 ratios that were considered, only those linear fits with a value of 0.90 for the correlation coefficient r (or $r^2 = 0.81$) were selected. The highlighted fission product ratios indicate those with an r^2 of 0.81 or higher. This criterion for the selection of fission product ratios will be further refined based on analyses performed in FY17.

APPENDIX C: ORNL SAFEGUARDS ACTINIDE CONCENTRATION CALCULATOR (SACC)

EMPLOYING BEDDINGFIELD METHODS FOR MIXTURES SCREENING

Additionally, Beddingfield's publication discussed a method for identifying parent fissile isotope from its short-lived fission product spectrum [4]. This is done by comparing two weighting factors listed in Equations C-1 and C-2. Each of these equations was applied to the 56 ratios listed in Appendix A and used together with Beddingfield's weighting factors to identify if the sample is a fissile mixture and provide a rough approximation on the Plutonium concentration. Beddingfield's methods in addition to the mixtures identification method were incorporated into a living Excel document (Figure C.1: ORNL Safeguards Actinide Concentration Calculator (SACC)) that is used to temporarily house calculation methodologies developed throughout this work. In equations (C-1) and (C-2), r_{obs} is the measured fission product photopeak ratio of the U+Pu mixture. Theoretical photopeak ratios were determined using ENDF/B-IV fission product yields and decay data for ^{235}U and ^{239}Pu (r_U and r_{Pu}).

$$W_U = \left(1 - \left|\frac{r_{obs} - r_U}{r_{Pu} - r_U}\right|\right)100\% \qquad \text{C-1}$$

$$W_{Pu} = \left(1 - \left|\frac{r_{obs} - r_{Pu}}{r_{Pu} - r_U}\right|\right)100\% \qquad \text{C-2}$$

While the excel spreadsheet serves as an example of how the DNDG analysis method may be automated to flag the presence of plutonium, there are important differences between the DNDG method and the Beddingfield method. In the Beddingfield approach, the photopeak ratios for ^{235}U and ^{239}Pu are calculated theoretically. The DNDG method uses measured photopeak ratios and the fraction of ^{239}Pu is determined based on an empirical calibration of photopeak ratios versus known ^{239}Pu fraction in ^{235}U+^{239}Pu mixtures. The measurement based approach reduces uncertainties associated with nuclear data, and is independent of theoretical assumptions regarding neutron spectral shape and magnitude, and decay characteristics of fission products.

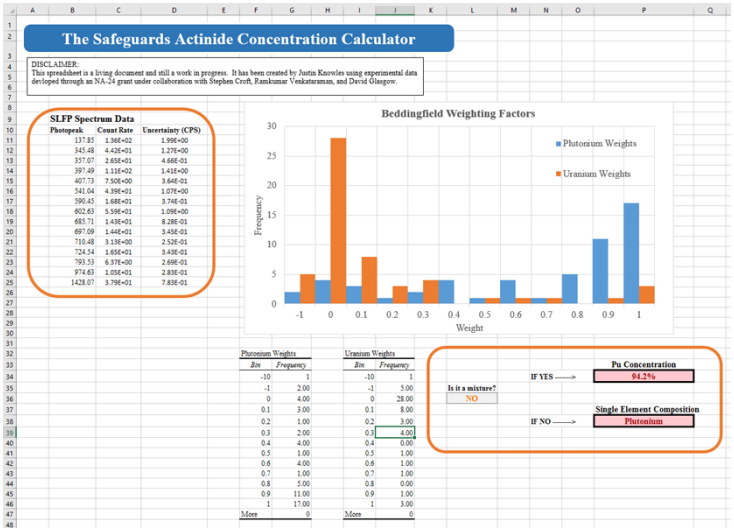

Figure C.1: ORNL Safeguards Actinide Concentration Calculator (SACC)

APPENDIX D: RESEARCH REACTORS IN NORTH AMERICA AND WESTERN EUROPE

Table D.1. Research Reactors in North America (Thermal Power of 6 MW or higher)

Country	Facility Name	Type	Thermal Power (kW)	Status
United States of America	MITR-II MASS. INST. TECH.	TANK	6000.0000	OPERATIONAL
United States of America	MURR Univ. of Missouri	TANK IN POOL	10000.0000	OPERATIONAL
United States of America	FAST BURST (FBR) White Sands	FAST BURST	10000.0000	OPERATIONAL
United States of America	NBSR (NIST)	HEAVY WATER	20000.0000	OPERATIONAL
United States of America	HT3R	HE COOLED	25000.0000	PLANNED
United States of America	HFIR (ORNL)	TANK	85000.0000	OPERATIONAL
Canada	NRU (National Research Universal reactor)	HEAVY WATER	135000.0000	OPERATIONAL
United States of America	ATR (Advanced Test Reactor, INL)	TANK	250000.0000	OPERATIONAL

Table D.2. Research Reactors in Western Europe (Thermal Power of 4 MW or higher)

Country	Facility Name	Type	Thermal Power (kW)	Status
Belgium	BR-1	GRAPHITE	4000.0000	OPERATIONAL
Germany	BER-II	POOL	10000.0000	OPERATIONAL
France	ORPHEE	POOL	14000.0000	OPERATIONAL
Germany	FRM II	POOL	20000.0000	OPERATIONAL
Norway	HBWR	HEAVY WATER	20000.0000	OPERATIONAL
France	CABRI	POOL	25000.0000	OPERATIONAL
Netherlands	HFR	TANK IN POOL	45000.0000	OPERATIONAL
France	HFR	HEAVY WATER	58300.0000	OPERATIONAL
Belgium	MYRRHA	FAST	85000.0000	PLANNED
France	RES	PWR	100000.0000	UNDER CONSTRUCTION
France	REACTOR JULES HOROWITZ	TANK IN POOL	100000.0000	UNDER CONSTRUCTION
Belgium	BR-2	TANK IN POOL	100000.0000	OPERATIONAL